Marine Environment
Research Centre

CNR ISMAR – Marine
Science Institute

MEDOCC 05

- Cruise Report -

24th April 2005 – 16th May 2005

CNR IBF - Istituto di
Biofisica

Università degli Studi di
Genova

SACLANT Undersea
Research Centre

Università degli Studi di Siena

Edited by K. Schröder

Table of Contents

Cruise Particulars

NAME	*MEDOCC 05*
DATES	*24^{TH} APRIL 2005 – 16^{TH} MAY 2005*
STUDY AREA	*LIGURIAN SEA*
	GULF OF LIONS
	BALEARIC SEA
	ALGERIAN BASIN
	CENTRAL MEDITERRANEAN SEA
	TYRRHENIAN SEA
HEAD OF MISSION	*MIRENO BORGHINI, CNR-ISMAR*
PARTICIPANT INSTITUTES	*ENEA – CRAM*
	CNR – ISMAR
	CNR – IBF
	UNIVERSITY OF GENOA
	UNIVERSITY OF SIENA
	SACLANT – UNDERSEA RESEARCH CENTRE
RESEARCH VESSEL	*URANIA*
DEPARTURE PORT	*LIVORNO*
ARRIVAL PORT	*CIVITAVECCHIA*

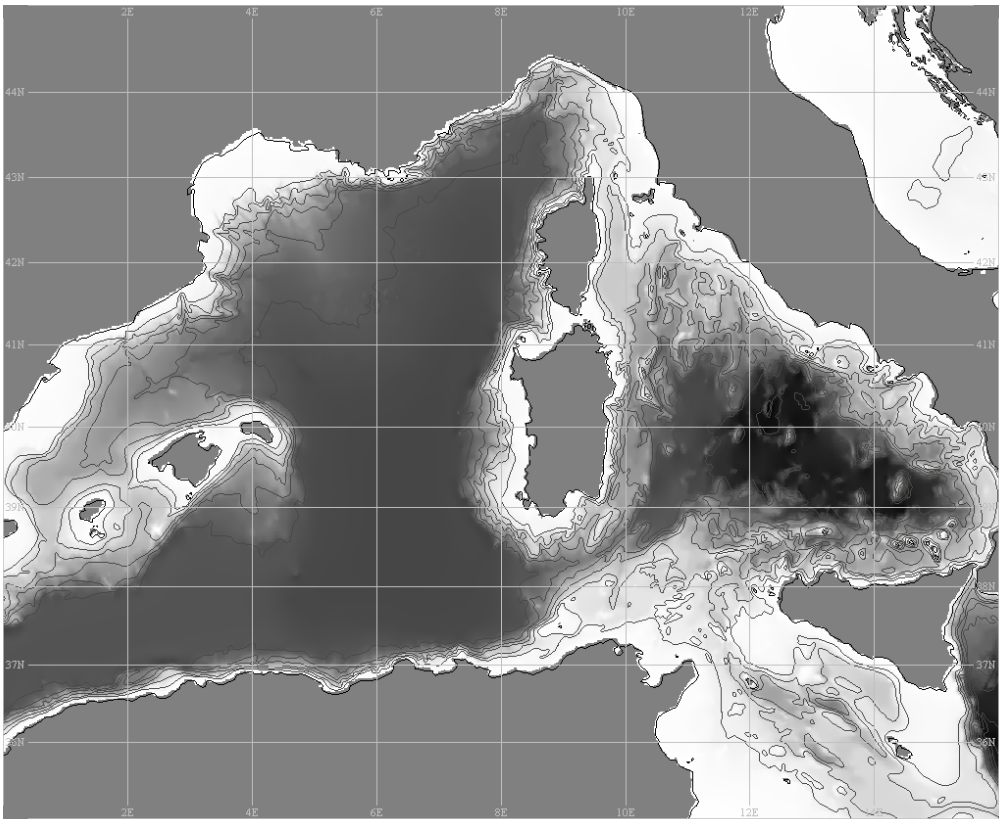

Scientific Staff

ENEA-CRAM

Marine Environment Research Centre P.O.BOX 224 19036 Pozzuolo di Lerici (SP) Italy phone: +39.0187.9781 fax: +39.0187.978236	Delfanti Roberta Torricelli Leonardo Tangherlini Michele Schröder Katrin	Researcher Researcher Researcher Researcher

CNR-ISMAR

c/o ENEA–Santa Teresa 19036 Pozzuolo di Lerici (SP) Italy phone: +39.0187.978300 fax: +39.0187.970585	Bacciola Domenico Borghini Mireno Negri Azzurra	Technician Technician Assistant

CNR-IBF

Via G. Moruzzi 1 San Cataldo 56124 Pisa Italy phone: +39.050.3152578/3 fax: +39.050.3152760	Nannicini Luciano Santinelli Chiara	Technician Researcher

UNIVERSITA' DI GENOVA

Via Balbi 5 16126 Genova Italy phone: +39.010.20991 fax: +39.010.2099227	Bertora Carlo Costa Eleonora Garibaldi Fulvio Lanteri Luca Palandri Giovanni Oliva Ida Russo Giorgia Siliceo Iniazio Viviani Lorenzo Fornaciari Elena	Student Student Researcher Researcher Researcher Student Student Student Student Student

UNIVERSITA' DI PISA

	Giorgio Serchi Francesco	Student

UNIVERSITA' DI SIENA

Via A. Moro 2 53100 Siena Italy phone: +39.0577.234373/4 fax: +39.0577.234177	Bracchini Luca Dattilo Arduino Massimo	Researcher Researcher

SACLANT

Viale San Bartolomeo 400 19138 La Spezia Italy phone: +39.0187.527.1 fax: +39.0187.527.700	Bassetti Mirco Ampolo Rella Marina	Researcher Student

Scientific objectives

This report presents the preliminary results obtained during the MEDOCC 05 cruise, carried out from 24th April – 16th May 2005, on board of the Italian R/V URANIA in the Western Mediterranean Sea.

The cruise was planned in order to achieve the following objectives:

1. Water mass properties and circulation features

- **to define the principal circulation paths and the physical-chemical-biological properties (temperature, salinity, oxygen, nutrients, dissolved organic carbon, colored dissolved organic matter, etc) of the superficial, intermediate and deep water masses in the central part of the Western Mediterranean Sea, through measurements along key sections located in the interior and at the boundaries of the basin;**
- **to select some transects with the purpose of performing long term surveys;**

2. Carbon cycle

- **to estimate the particulate carbon export from the photic zone in some significant stations and the relationship to hydrology and biological parameters;**
- **to investigate the linkage between the quantities and qualities of DOC and CDOM (e.g. specific absorbance, spectral slope and specific spectral slope) and to study the interactions of these parameters with the spectral irradiance in the water column;**
- **to study the optic characteristics of the water column in the visible and UV solar bands, to measure UV-B, UV-A and PAR radiation on the water surface, to evaluate reflectance on the water surface;**
- **to quantify and classify phytoplanktonic populations;**
- **to measure the sedimentation rate in three key areas;**

3. Cetacean Research

- **to study cetacean communities and to map the distribution of mesopelagic fauna related both to the presence of cetaceans and to hydrology in the Ligurian–Provencal Basin;**

4. Methodological development

- **to use conventional techniques to calibrate acoustic backscatter data obtained using an Acoustic Doppler Current Profilers, to derive estimates of suspended solids concentration on the column water;**
- **to compare different chlorophyll quantification methods and to calibrate the fluorimeter coupled with the CTD-probe with different photochemical techniques.**

Scientific Background

General description

This cruise has been planned to investigate the central part of the Western Mediterranean Sea. We will try to better define the pathway and the properties of the water masses involved in the circulation of this basin and to assess the carbon export from the photic zone to the deep layers. The focus was on defining the characteristics of:

- the **inflowing water masses**, which are involved in the dense water formation processes (Modified Atlantic Water from the Ligurian Sea; Levantine Intermediate Water and Tyrrhenian Deep Water, coming from the Tyrrhenian Sea);
- the **newly formed water masses** which exit the basin (Winter Intermediate Water and Western Mediterranean Deep Water);
- the **southern current** (Modified Atlantic Water and re-circulated Levantine Intermediate Water) which apparently are not involved in the above mentioned processes.

Furthermore the processes involved in the dense water formation allow the replenishment of nutrients into the upper layer, followed by a bloom with locally high primary production rates and high carbon export from the photic zone to the deep layers. Another important aspect is the difference in carbon export between a mesotrophic area (Gulf of Lions in spring) and the oligotrophic ones in the rest of basin. The role of oligotrophic areas in overall export production is probably not very important, because the greatest part of photosynthesised carbon is recycled in the surface layer and raplidy re-excanged with the atmosphere.

The cruise approach takes into account a possible reiteration of the survey in the following years in order to evaluate the interannual variability of the basin's conditions and its role in climatic processes. Therefore we have defined a series of key section, both in the interior of the basin and on its boundaries. The sections have been chosen to be able to intercept every inflowing and outflowing water mass. Previous studies have indicated that the most suitable section for this purpose are:

- the **Sardinian Channel**
- between **Corsica and France**
- between **Majorca and Sardinia**

} these sections catch the water masses that are involved in the dense water formation processes

- through the **Gulf of Lions** — the dense water formation area

- between **Majorca and Spain**
- between **Majorca and Algeria**

these sections catch the newly formed water masses

A long term survey in these sections could provide significant information about the reasons of the trends observed in the deep waters of this basin (increased salinity and temperature): climatic processes (dense water formation), anthropogenic processes (damming of the main rivers) and/or physical processes (warmer water originated in the Eastern Mediterranean Sea).
A further relevant question is if there is a related trend even in the chemical and biological characteristics of the involved water masses.
The central part of the Western Mediterranean Sea plays an important role in the circulation of the whole Mediterranean Sea, because of the presence, in its northern part, of dense water formation areas.
The **Ligurian–Provencal Basin**, along with the **Gulf of Lions** and the **Balearic Sea**, forms the North-western Mediterranean Basin. This region is characterized by a general cyclonic circulation involving both the surface layer of Modified Atlantic Water (MAW) and the Levantine Intermediate Water (LIW) layer below. In winter, these basins are sites of important dense water formation processes capable of triggering convective flows within the water column (Gasparini et al., 1999). The processes are particularly intense in the Gulf of Lions (MEDOC Group, 1970; Leaman and Schott, 1991), even though they have also been reported in the Balearic Sea (Salat and Font, 1987) as well as in the central part of the Ligurian Basin (Sparnocchia et al., 1995). In these basins, however, due to the less severe weather conditions, cooling and mixing are less intense and only involve the MAW layer. They lead to the formation of a Winter Intermediate Water (WIW), which is a cooled and mixed MAW that reaches the buoyancy equilibrium between the MAW and the LIW layers. The WIW formation was observed both in the basin interior along the coastal zone and different sinking mechanisms have been proposed.
The **Gulf of Lions** is mainly characterised by a permanent cyclonic circulation and manifests strong seasonal variations of the physical and biochemical properties due to convective movements and deep mixing during the wintertime (Millot, 1999). In winter, the deep convection sets the homogenisation of the water column bringing saline water from the intermediate layer close to the surface. In the Gulf of Lions, the highest surface phytoplankton

biomass develops in winter and spring due to the violent mixing and vertical injections of nutrient rich deep waters in the open-sea convective region.

In the **Algerian Basin** the MAW flow forms what is now commonly named the "Algerian Current" (Millot, 1985). This current is relatively narrow (30–50 km) and deep (200–400 m at the coast) near 0°E, but it becomes wider and thinner while progressing eastward (Benzohra and Millot, 1995). Its unstable character sometimes leads to the generation of meanders a few tens of km in wavelength, but the current continues flowing along the Algerian slope till the Channel of Sardinia (Morel and Andre, 1991). The mesoscale eddies in the Algerian Basin induce intense currents over the whole deeper layer and even close to the bottom (Millot et al., 1997).

The **Central Mediterranean** is characterised by a very complicated bottom topography, which directly affects the water exchange between the two Mediterranean basins (western and eastern Mediterranean Sea). The most salient features are the unequal depths of the boundary sections (Astraldi et al., 2002). In the Sardinia Channel (section D13-D21 in Figure 1), the silldepth is at about 1900 m, allowing the free exchange of the deep waters with the WMED, but in the Sicily Strait (section 410-432), the deeper sill is at about 430 m, thus imposing strong constraints on the exchanges with the EMED. In between, a wide area of very shallow waters off Tunisia provides a further obstacle to a direct connection between the two basins. All water masses outflowing at depth, both from the WMED (Krivosheya and Ovchinnikov, 1973; Hopkins, 1988) and from the EMED (Astraldi et al., 1996), are conveyed into the **Tyrrhenian Sea**, an intermediate basin whose southern part strongly interacts with the central Mediterranean. Section 212-291 is substantially formed by two main channels with a wide plateau in between. The deeper one, in the central part, directly connects the Tyrrhenian Sea with the Sardinia Channel and the WMED, and the other, adjacent to the Sicilian slope, connects, with an increasing depth, the Sicily Strait with the Tyrrhenian Sea.

Hence, this study area is a very complex system, with even extreme climatic conditions in its northern part and an almost sub-tropical climate in its southern part. It sustains one of the most productive areas of the whole Mediterranean Sea, with the vastest marine mammals and large fishes community.

Further interesting aspects regard the hydrological properties (temperature and salinity) of the deep and intermediate layers, which have presented a positive trends for some decades. The reasons of this trend are not yet known. Furthermore, the water masses coming from this area constitute the principal source of the outflowing Mediterranean water at Gibraltar.

An increased knowledge about all these aspects will permit a more complete understanding of the role and the functioning of the Western Mediterranean Sea.

State of the knowledge

Previous studies in this area have focused on the dense water formation process and on the extension and evolution of the eddies in the southern part, while they have neglected the circulation features and the variability of the water masses induced by such processes. Even if the principal characteristics and the general circulation scheme are known for this area, it is necessary to clarify many aspects of the path and of the regulating mechanisms for each water mass.

Some important detailed studies of the basin have regarded only the distinctive events. For instance, the dense water formation processes occurring in winter in the Gulf of Lions and in the Ligurian Sea have been extensively studied, both experimentally and through models.

Only recently more attention has been given to the productivity of the area and its relationship with the prevailing circulation processes. Also the southern part of the basin has been intensely studied. This area is characterized by anticyclonic eddies which move along the African coast toward the Sardinian Channel.

Further, some important Spanish studies have regarded the Catalan Sea.

Nevertheless, the circulation of the water masses and the variability of their physical, chemical and biological properties are substantially unidentified, because till now no wide-ranging approach has been adopted.

Cruise Plan

The following table summarizes the parameters that have been measured and the sampling group involved in the operation, while table 2 lists the sampling equipment and the methods of analysis.

Parameter/Instrument	**Sampling Group**
CTD/O2/rosette	CNR-ISMAR - ENEA
Salinity	CNR-ISMAR
XBT	CNR-ISMAR
Dissolved Oxygen	CNR-ISMAR
NO3, P04, SiO4	CNR-ISMAR – ENEA
Chlorophyll	CNR-ISMAR – ENEA – Saclant
Sediment	ENEA
Th-234	ENEA
Cs-137	ENEA
Pb-210	ENEA
Phytoplankton	ENEA
Mesopelagic fauna	University of Genoa
DOC	CNR-IBF
POC	ENEA
TSS	ENEA – Saclcant
Spectroradiometer	University of Siena

Table 1 Measured Parameters

Small-Volume Sampling	General Oceanics 24-place rosette with 10-liter bottles
CTD System	CTD SBE 911 plus
XBT	T4, T5 and Deep Blue (Sippican Inc.)
Salinometer	AUTOSAL
Oxygen	Winkler titration
Nutrients	Samples only, no on board analyses
Chlorophyll	Filtration
Sediment	Box corer
Th-234	*In situ* CHALLENGER OCEANICS pumps, sediment samples
Cs-137	Water samples and preconcentration, sediment samples
Pb-210	Sediment samples only
Phytoplankton	Net cast
Mesopelagic fauna	ISAACS KIDD trawl
DOC	Filtration
POC	Filtration
TSS	Filtration
Solar spectra transmission	Spectroradiometer EPP2000C (StellarNet Inc)

Table 2 Sampling equipment and analysis methods

The track is shown in Figure 1. We planned to spend 23 days at sea. The geographic boundaries of the survey are 37.00 °N - 43.75 °N latitude and 1.93 °E - 12.33 °E longitude. After leaving Livorno, the cruise began on the 24th April with a CTD/rosette section across the Ligurian Sea (900-913). Operations included subsurface tows using an ISAACS KIDD Midwater Trawl (IKMT) for mesopelagic fauna sampling. Next, another set of stations has been covered with CTD/rosette and IKMT (52-60B) in the same region. After these stations, the IKMT staff got off and the ENEA staff has embarked. Next, URANIA began another CTD/rosette section (L1-L14) across the Gulf of Lions, a dense water formation area. In the middle of the section, a complete station will be performed. A “complete station” includes the following operations: CTD/rosette (nutrients, chlorophyll, POC, DOC, TSS), sediment sampling with a box corer, Th-234 sampling with *in situ* pumps, Cs-137 in seawater, phytoplankton net cast. Subsequently, the vessel headed westward to begin a CTD/rosette section through the Balearic Sea (B1-B8). It bypassed Majorca Island and began the CTD/rosette section toward Algeria (D1-D12). In the middle of the section, another complete station has been performed (D8). At point D12, URANIA turned to reach section S1-S21. During the way we launched XBTs. A complete station was sampled even in the middle of the S1-S21 section, precisely at point S12.

Further we moved toward the next CTD/rosette section across the Sardinian Channel (D13-D21). In the middle of the Channel we carried out another complete station (D16).

The next CTD/rosette sections are located respectively in the Sicily Channel (405-438) and in the Sardinia-Sicily Channel (212-291).

To finish, URANIA entered the Tyrrhenian Sea, where we have launched XBT and stopped at four CTD/rosette stations, one of which was a complete station, excluding sediment sampling (A9).

We arrived on the 16th May in the port of Civitavecchia.

The station list is shown in table 3.

Cruise Maps

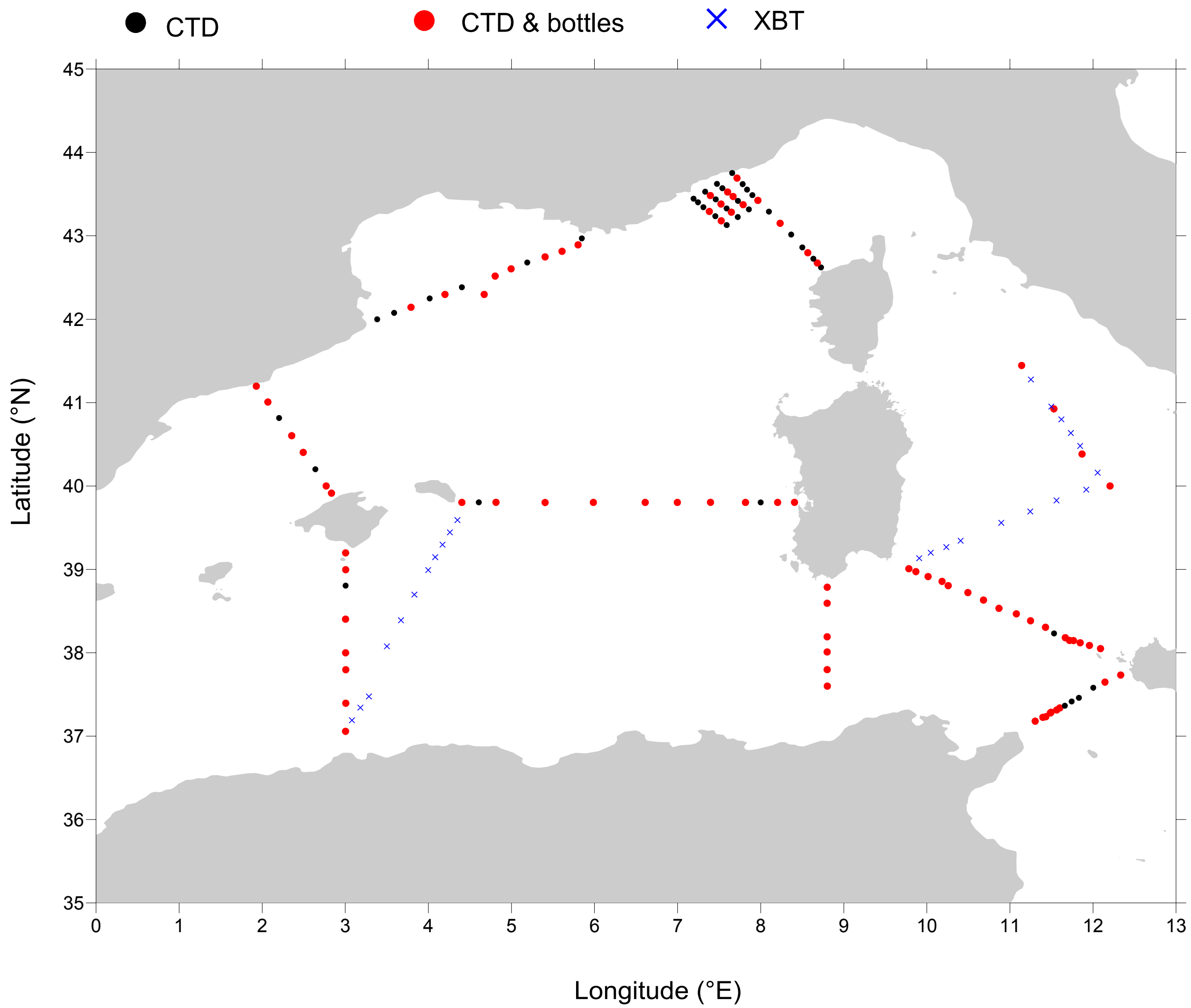

Figure 1 Cruise map

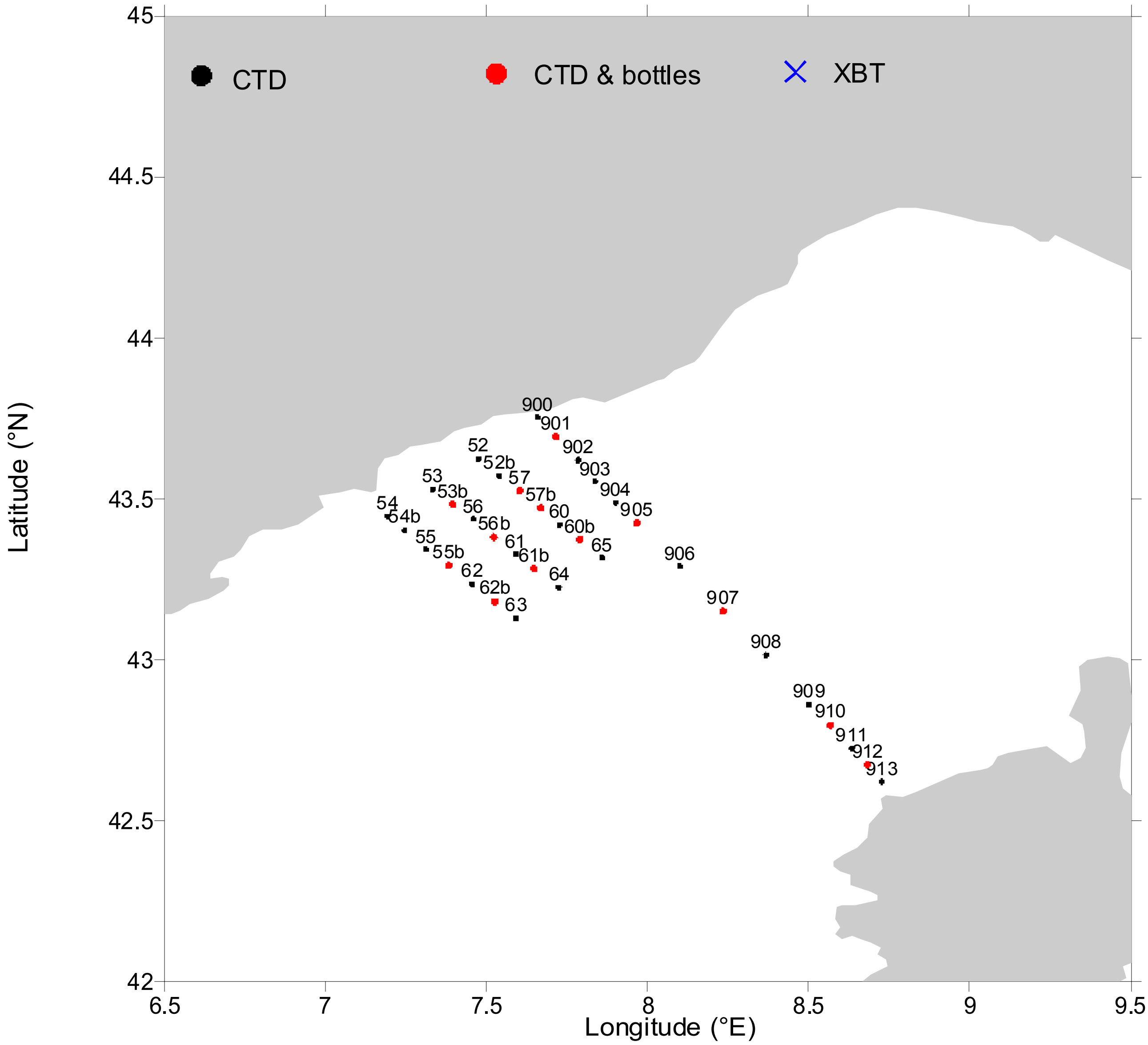

Figure 2 First set of stations in the Ligurian-Provencal Basin

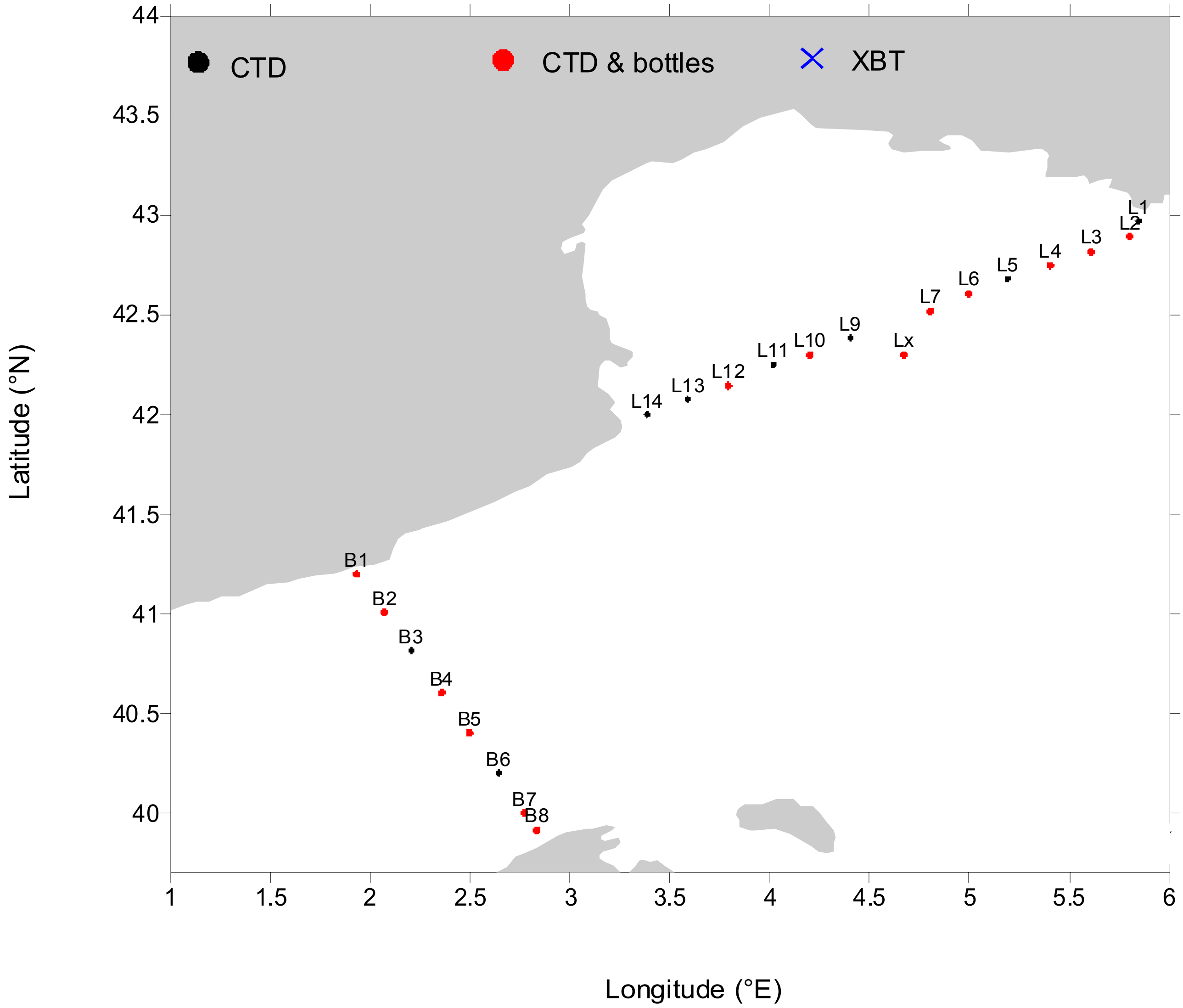

Figure 3 Second set of stations in the Gulf of Lions and the Balearic Sea

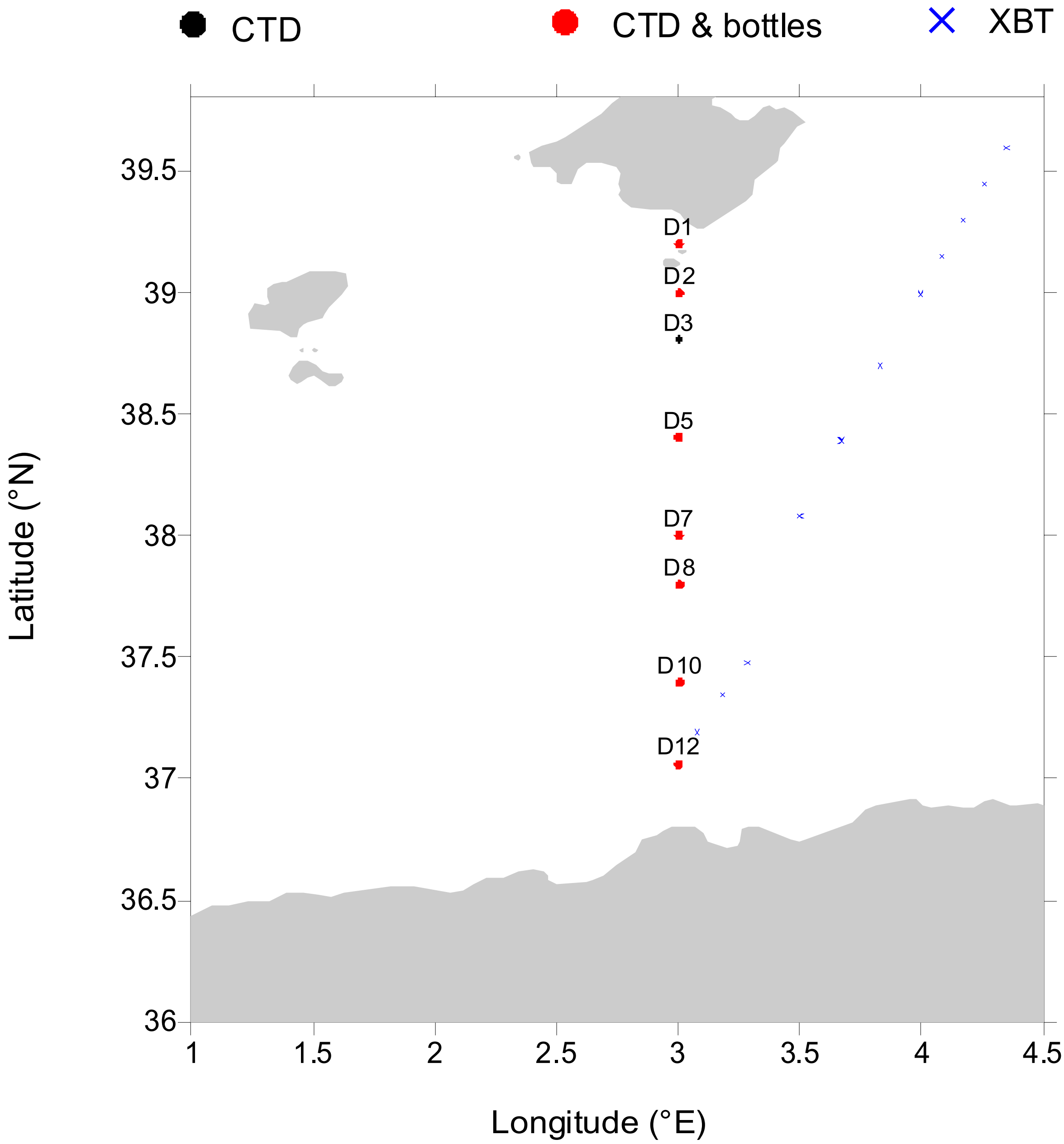

Figure 4 Third set of stations in the Algerian Basin

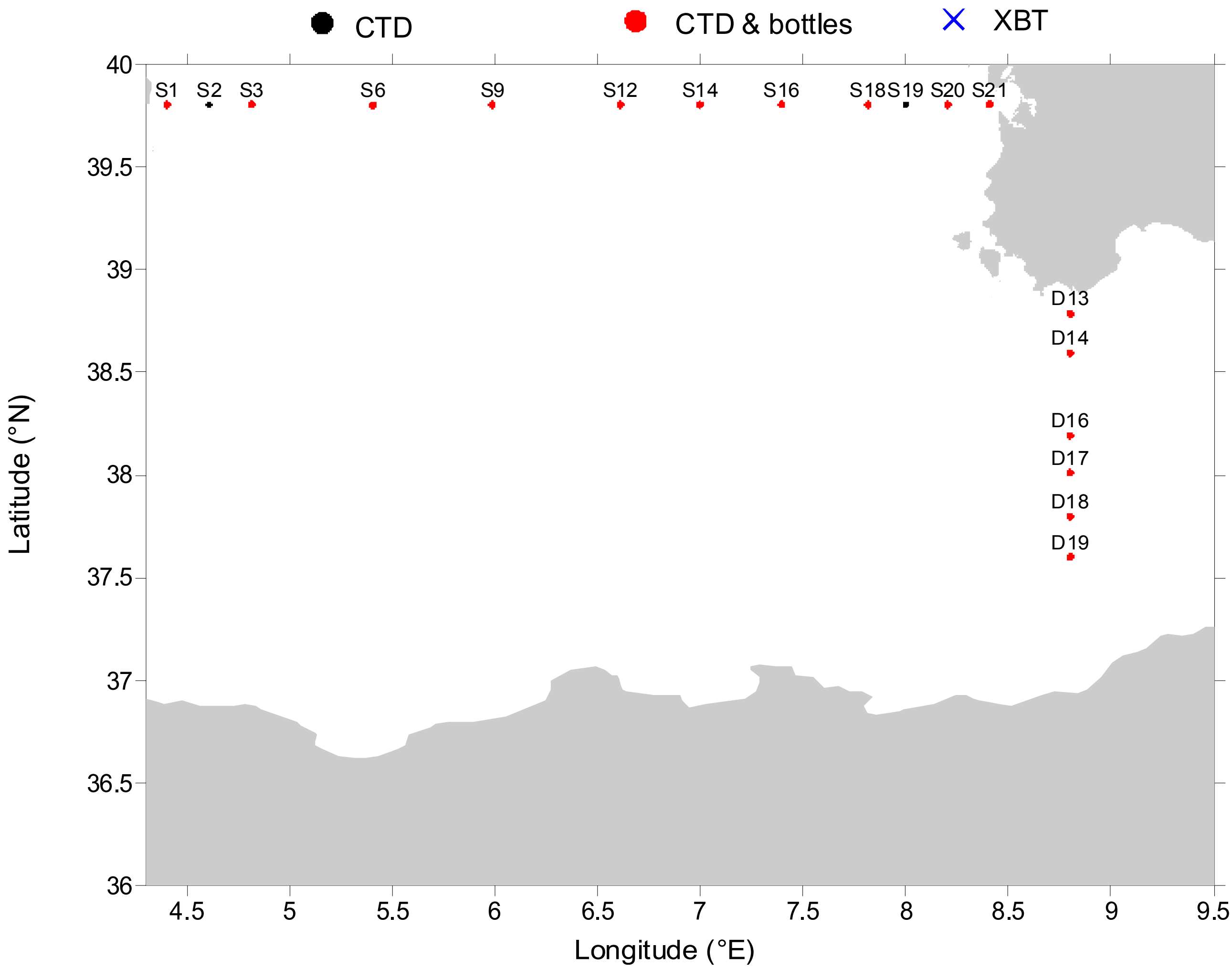

Figure 5 Fourth set of stations in the Algerian Basin and Sardinian Channel

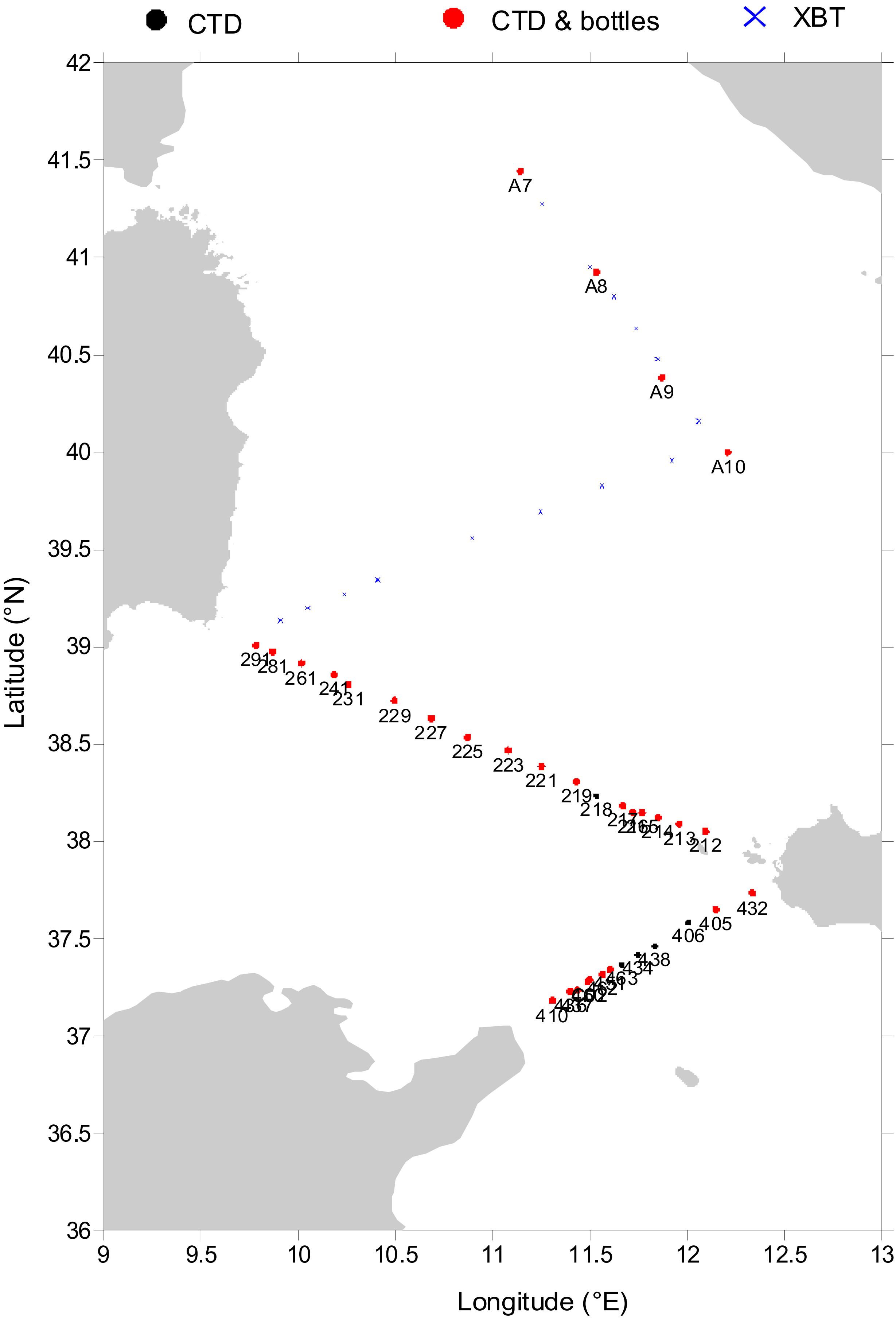

Figure 6 Fifth set of stations in Central Mediterranean Sea and Tyrrhenian Sea

Cruise Stations

Station	Date	Long (°E)	Lat (°N)	Depth (m)	Type
913	25/04/2005	8.726	42.621	253	CTD
912	25/04/2005	8.682	42.674	1083	CTD, oxygen, salinity, nutrients, chlorophyll, DOC,light
911	25/04/2005	8.634	42.725	1740	CTD
910	25/04/2005	8.567	42.797	2273	CTD, oxygen, salinity, nutrients, chlorophyll, DOC,light
909	25/04/2005	8.501	42.861	2610	CTD
908	25/04/2005	8.367	43.015	2600	CTD
907	26/04/2005	8.234	43.15	2546	CTD, oxygen, salinity, nutrients, chlorophyll, DOC
906	26/04/2005	8.099	43.29	2500	CTD
905	26/04/2005	7.966	43.425	2400	CTD, oxygen, salinity, nutrients, chlorophyll, DOC, light, net cast
904	26/04/2005	7.9	43.488	2423	CTD
903	26/04/2005	7.836	43.554	2331	CTD
902	26/04/2005	7.783	43.62	2133	CTD
901	26/04/2005	7.715	43.692	1130	CTD, oxygen, salinity, nutrients, chlorophyll, DOC
900	27/04/2005	7.657	43.753	294	CTD
52	27/04/2005	7.474	43.623	1240	CTD
52b	27/04/2005	7.539	43.571	1980	CTD
57	27/04/2005	7.602	43.525	2210	CTD, nutrients
57b	27/04/2005	7.668	43.471	2285	CTD, nutrients, chlorophyll
60	27/04/2005	7.726	43.419	2314	CTD
60b	27/04/2005	7.789	43.373	2279	CTD, nutrients, chlorophyll, DOC, net cast
65	27/04/2005	7.858	43.317	2400	CTD
64	27/04/2005	7.724	43.225	2460	CTD
63	27/04/2005	7.591	43.129	2517	CTD
62b	27/04/2005	7.525	43.18	2448	CTD, nutrients, chlorophyll
62	28/04/2005	7.454	43.235	2338	CTD
55b	28/04/2005	7.382	43.292	2341	CTD, nutrients, chlorophyll
55	28/04/2005	7.31	43.343	2250	CTD
54b	28/04/2005	7.245	43.402	1870	CTD
54	28/04/2005	7.192	43.445	1612	CTD
53	28/04/2005	7.332	43.529	1685	CTD

Station	Date	Long (°E)	Lat (°N)	Depth (m)	Type
53b	28/04/2005	7.394	43.483	1924	CTD, oxygen, salinity, nutrients, chlorophyll, net cast
56	28/04/2005	7.459	43.437	2058	CTD
56b	29/04/2005	7.522	43.381	2000	CTD, nutrients, chlorophyll
61	29/04/2005	7.59	43.328	2155	CTD
61b	29/04/2005	7.647	43.283	2267	CTD, nutrients, chlorophyll
L1	30/04/2005	5.847	42.969	400	CTD
L2	30/04/2005	5.802	42.892	2083	CTD, nutrients, chlorophyll, DOC, TSS, net cast
L3	30/04/2005	5.609	42.814	2216	CTD, TSS
L4	01/05/2005	5.405	42.747	1833	CTD, nutrients, chlorophyll, DOC, net cast
L5	01/05/2005	5.19	42.68	1870	CTD
L6	01/05/2005	4.996	42.604	1770	CTD, nutrients, chlorophyll, light
L7	01/05/2005	4.804	42.517	1630	CTD, light
Lx	01/05/2005	4.672	42.297	2011	CTD, nutrients, chlorophyll, DOC, TSS, POC, Caesium-137, Thorium-234, light, net cast
L9	01/05/2005	4.403	42.383	1890	CTD
L10	02/05/2005	4.2	42.297	1794	CTD, nutrients, chlorophyll, DOC, TSS
L11	02/05/2005	4.016	42.249	1502	CTD
L12	02/05/2005	3.791	42.143	1200	CTD, nutrients, chlorophyll, DOC
L13	02/05/2005	3.588	42.076	894	CTD, light
L14	02/05/2005	3.384	41.999	151	CTD
B1	02/05/2005	1.929	41.197	42	CTD, TSS, light
B2	02/05/2005	2.068	41.007	910	CTD, nutrients, chlorophyll, DOC, TSS, light, net cast
B3	02/05/2005	2.203	40.815	1528	CTD
B4	02/05/2005	2.355	40.603	1871	CTD, nutrients, chlorophyll, DOC
B5	03/05/2005	2.494	40.403	1865	CTD, oxygen, salinity, nutrients, chlorophyll, DOC
B6	03/05/2005	2.64	40.201	1730	CTD, light
B7	03/05/2005	2.77	40	1324	CTD, nutrients, chlorophyll, DOC, TSS, light, net cast
B8	03/05/2005	2.834	39.914	85	CTD, TSS, light
D1	03/05/2005	3.004	39.198	40	CTD, TSS, light
D2	03/05/2005	3.005	38.996	1278	CTD, nutrients, chlorophyll, TSS
D3	03/05/2005	3.004	38.805	2452	CTD

Station	Date	Long (°E)	Lat (°N)	Depth (m)	Type
D5	03/05/2005	3.003	38.403	2660	CTD, nutrients, chlorophyll, DOC
D7	04/05/2005	3.004	38	2776	CTD, Caesium-137, light
D8	04/05/2005	3.006	37.797	2775	CTD, nutrients, chlorophyll, DOC, POC, TSS, light, Thorium-234, Sediment
D10	04/05/2005	3.006	37.395	2745	CTD, oxygen, salinity, nutrients, chlorophyll, DOC
D12	04/05/2005	3.003	37.058	2634	CTD, nutrients, chlorophyll, DOC
S1	07/05/2005	4.403	39.803	105	CTD, TSS, light
S2	07/05/2005	4.607	39.804	1306	CTD, light
S3	07/05/2005	4.814	39.804	2375	CTD, oxygen, salinity, nutrients, chlorophyll, DOC, light
S6	07/05/2005	5.405	39.802	2794	CTD, oxygen, salinity, nutrients, chlorophyll, DOC
S9	07/05/2005	5.986	39.803	2815	CTD, nutrients, DOC
S12	08/05/2005	6.61	39.803	2825	CTD, POC, TSS, light, Caesium-137, Thorium-234, net cast, Sediment
S14	08/05/2005	6.997	39.803	2811	CTD, oxygen, salinity, nutrients, chlorophyll, DOC, POC, TSS
S16	08/05/2005	7.396	39.804	2742	CTD, oxygen, salinity, nutrients, chlorophyll, DOC, net cast
S18	08/05/2005	7.817	39.803	1641	CTD, nutrients, chlorophyll, DOC
S19	09/05/2005	8	39.803	886	CTD
S20	09/05/2005	8.204	39.803	100	CTD, TSS
S21	09/05/2005	8.407	39.804	45	CTD, TSS
D13	09/05/2005	8.801	38.786	125	CTD, TSS, light
D14	09/05/2005	8.8	38.594	698	CTD, nutrients, chlorophyll, DOC, TSS, light
D16	09/05/2005	8.8	38.192	2234	CTD, nutrients, chlorophyll, DOC, POC, TSS, Caesium-137, Thorium-234, net cast, Sediment
D17	10/05/2005	8.8	38.01	1660	CTD, oxygen, salinity, nutrients, chlorophyll
D18	10/05/2005	8.8	37.798	1400	CTD, light
D19	10/05/2005	8.802	37.6	499	CTD, nutrients, chlorophyll, TSS, light
410	10/05/2005	11.304	37.18	248	CTD, nutrients, chlorophyll, DOC, TSS
436	11/05/2005	11.396	37.226	413	CTD, TSS
437	11/05/2005	11.432	37.233	439	CTD, TSS

Station	Date	Long (°E)	Lat (°N)	Depth (m)	Type
460	11/05/2005	11.486	37.278	543	CTD, TSS
462	11/05/2005	11.562	37.314	90	CTD, TSS
C02	11/05/2005	11.494	37.286	535	CTD, nutrients, chlorophyll, DOC, Caesium-137, light, net cast, mooring maintenance
451	11/05/2005	11.6	37.339	540	CTD, nutrients, chlorophyll, DOC, net cast, light
463	11/05/2005	11.661	37.365	92	CTD
434	11/05/2005	11.743	37.416	85	CTD
438	11/05/2005	11.83	37.46	75	CTD
433	11/05/2005	11.922	37.515	105	CTD, nutrients, chlorophyll, DOC
406	11/05/2005	12.003	37.581	149	CTD
405	11/05/2005	12.144	37.648	97	CTD, nutrients, chlorophyll, DOC
432	11/05/2005	12.333	37.733	168	CTD, nutrients, DOC
212	12/05/2005	12.09	38.05	220	CTD, TSS
213	12/05/2005	11.957	38.088	410	CTD, TSS
214	12/05/2005	11.846	38.12	1160	CTD, oxygen, salinity, nutrients, TSS
215	12/05/2005	11.765	38.146	1200	CTD, nutrients, chlorophyll, light
216	12/05/2005	11.717	38.148	951	CTD, Caesium-137
217	12/05/2005	11.666	38.181	762	CTD, nutrients, net cast, chlorophyll, DOC,light
218	12/05/2005	11.531	38.232	229	CTD, light
219	12/05/2005	11.428	38.306	890	CTD, nutrients, light
221	12/05/2005	11.248	38.384	686	CTD, nutrients, light
223	12/05/2005	11.077	38.467	840	CTD, nutrients, chlorophyll, DOC
225	12/05/2005	10.868	38.533	730	CTD, nutrients
227	12/05/2005	10.682	38.632	1541	CTD, nutrients
229	12/05/2005	10.494	38.722	2460	CTD, nutrients, chlorophyll, DOC
231	13/05/2005	10.257	38.805	2316	CTD, oxygen, salinity, nutrients
241	13/05/2005	10.183	38.856	2525	CTD, Caesium-137
261	13/05/2005	10.015	38.914	1500	CTD, nutrients, light
281	13/05/2005	9.868	38.973	1330	CTD, nutrients, chlorophyll, DOC, light
291	13/05/2005	9.783	39.008	1004	CTD, nutrients, TSS, light
A10	14/05/2005	12.205	40	3600	CTD, oxygen, salinity, nutrients, DOC

Station	Date	Long (°E)	Lat (°N)	Depth (m)	Type
A9	14/05/2005	11.868	40.383	2686	CTD, nutrients, chlorophyll, DOC, light, Thorium-234 (2000 m)
A8	14/05/2005	11.529	40.925	2320	CTD, nutrients, chlorophyll, DOC
A7	14/05/2005	11.141	41.445	1033	CTD, nutrients, chlorophyll, DOC, net cast
T4_00006	05/05/2005	3.501	38.0774	-	XBT
T4_00007	05/05/2005	3.6704	38.3899	-	XBT
T4_00008	05/05/2005	3.8321	38.6974	-	XBT
T4_00010	05/05/2005	3.998	38.9926	-	XBT
T4_00014	05/05/2005	4.3499	39.5912	-	XBT
TD_00002	05/05/2005	3.0802	37.1906	-	XBT
TD_00003	05/05/2005	3.1822	37.3427	-	XBT
TD_00004	05/05/2005	3.2846	37.4767	-	XBT
TD_00011	05/05/2005	4.0823	39.1465	-	XBT
TD_00012	05/05/2005	4.1703	39.2961	-	XBT
TD_00013	05/05/2005	4.2597	39.444	-	XBT
T4_00020	13/05/2005	10.4068	39.3438	-	XBT
T4_00022	13/05/2005	10.8953	39.5587	-	XBT
T4_00023	13/05/2005	11.2443	39.6943	-	XBT
T4_00024	13/05/2005	11.5608	39.8267	-	XBT
TD_00017	13/05/2005	9.9078	39.1338	-	XBT
TD_00018	13/05/2005	10.0468	39.1996	-	XBT
TD_00019	13/05/2005	10.2344	39.2669	-	XBT
TD_00025	13/05/2005	11.9192	39.9561	-	XBT
T4_00026	14/05/2005	12.0555	40.1595	-	XBT
T4_00028	14/05/2005	11.8452	40.4804	-	XBT
T4_00029	14/05/2005	11.7333	40.6353	-	XBT
T4_00030	14/05/2005	11.619	40.7995	-	XBT
T4_00031	14/05/2005	11.4981	40.9521	-	XBT
T4_00033	14/05/2005	11.2526	41.2767	-	XBT

Table 3 Station list

Sampling Strategy

The stations have been selected mainly based on previous knowledge and available literature. The sections have been chosen to be able to intercept every inflowing and outflowing water mass.

The hydrological characteristics of the study area have been determined by **CTD cast**. The CTD profiles were analysed onboard to precisely define the sampling depth along the water column.

In order to utilize **nutrients** and **Dissolved Organic Carbon (DOC)** as non-conservative tracers of the water masses, it was decided to take nutrients and DOC samples with a good spatial resolution (almost 55% of the hydrological casts), at the standard depths.

Samples for **chlorophyll** analysis were taken at 40% of the hydrological casts; generally, 2 samples were taken below the Deep Chlorophyll Maximum (DCM), detected by the fluorescence sensor on the CTD system, 1 sample at the DCM and 2 samples above the DCM.

Thorium-234 samples were collected in 5 significant stations: Lx, D8, S12, D16 and A9. SeaWIFS Satellite images suggested the presence of a productive area in the gyre off the Gulf of Lions, so station Lx was chosen to quantify the sinking flux of organic carbon and other particle associated elements from the photic zone in a productive area. The other stations (D8, S12 and D16) were chosen in the middle of the transects, in order to obtain a general basin-wide description of the carbon export processes. To evaluate the carbon and other particle export from the photic zone, in the same stations we sampled for **Particulate Organic Carbon (POC)** and for **Total Suspended Solids (TSS)**; in addition we took **sediment** cores, to evaluate the sedimentation rate in three key areas.

Caesium-137 is used as a conservative water mass tracer, so the stations were chosen in order to detect the paths of the principal water masses in the study area. Further, time-series of this tracer are available for the stations we have chosen, so we will be able to detect long term variability of the intercepted water masses.

Onboard Operations

CTD casts

At all the hydrological stations, pressure (P), salinity (S), potential temperature (θ) and dissolved oxygen concentration (DO) were measured with a CTD-rosette system consisting of a CTD SBE 911 plus, and a General Oceanics rosette with 24 12-l Niskin Bottles. Temperature measurements were performed with a SBE-3/F thermometer, with a resolution of 10^{-3} °C, and conductivity measurements were performed with a SBE-4 sensor, with a resolution of 3 x 10^{-4} S/m. In addition, salinities of water samples were analysed on board using a Guildline Autosal salinometer. Dissolved oxygen was measured with a SBE-13 sensor (resolution 4.3 µM), and data were checked against Winkler titration. The vertical profiles of all parameters were obtained by sampling the signals at 24 Hz, with the CTD/rosette going down at a speed of 1 m/s. The data were processed on board, and the coarse errors were corrected.

Nutrients

Seawater samples for nutrient measurements were collected at different depths, when the system CTD/rosette was going up, according to the vertical profiles of salinity, potential temperature and dissolved oxygen, recorded in real time. No filtration was employed, nutrient samples were stored at –20°C and nitrate, orthosilicate and ortophosphate concentrations will be determined later in the laboratory, using a hybrid Brän–Luebbe AutoAnalyzer following classical methods (Grasshoff et al., 1983) with slight modifications.

Laboratory: ENEA-CRAM

Chlorophyll

For chlorophyll analysis, 3 litres (in some stations 5 litres) of seawater were collected at definite depth above and below the Deep Chlorophyll Maximum (DCM), detected by the fluorescence sensor on the CTD system, and immediately filtered on 0.45 µm membrane (cellulose acetate, 47 mm) under gently vacuum. Then the filter was frozen at –20 °C. Analysis with the spectrophotometer will be performed in the laboratory on land.

Laboratory: ENEA-CRAM

Dissolved Organic Carbon (DOC)

Seawater samples for DOC measurements were collected at different depths, during the CTD/rosette up cast, according to the vertical profiles of salinity, potential temperature and dissolved oxygen, recorded in real time. They were immediately filtered on board, through sterile 0.2 µm membrane filters (Sartorius, Minisart, SM16534 K) under low N_2 pressure and stored in amber glass bottles at 4 °C in the dark until the analysis. The conditioning of the filters was performed by rinsing with a 200 ml aliquot of the seawater to be collected. DOC measurements will be carried out, in the laboratory ashore, with a Shimadzu 5000 TOC Analyser, equipped with quartz combustion column with 1.2% Pt on silica pillows of approximately 2 mm diameter (Santinelli et al., 2002).

Laboratory: CNR-IBF

Particulate Organic Carbon (POC)

A volume of 1-5 litres of seawater were collected at different depths above and below the Deep Chlorophyll Maximum (DCM) and immediately filtered through pre-ignited (450 °C) 0.7 µm glass fiber filters (25 mm Ø) under slight vacuum. Then the filter was frozen at –20 °C. Analysis will be performed in the laboratory on land with a CHN Analyzer (Grasshoff et al., 1983).

Laboratory: ENEA-Brasimone

Total Suspended Solids (TSS)

For TSS analysis, 1-5 litres of seawater were collected at the same depths as POC samples. In those stations where TSS quantity was supposed to be high (nearby the coast) the depth range of the ADCP was explored more in detail. Samples were immediately filtered on 0.45 µm membrane (cellulose acetate, 47 mm) under gently vacuum. Then the filter was frozen at –20 °C. Weighing of the filters for the TSS determination will be performed in the laboratory on land.

Laboratories: ENEA-CRAM, Saclant

Sediment cores

Sediment samples were collected by a modified Reineck box corer, carrying two core tubes:

- a cylindrical one (20 cm Ø) large enough to minimize the effect of shortening during penetration into the sediment;

- one with rectangular section (10 x 20 cm), for X-ray of the core.

The maximum length of the collected samples was 25 cm.

The cylindrical cores were sectioned directly onboard in slices 1 cm thick. The outer 1 cm ring of each slice was discarded to avoid the effect of downtraining of surface material towards deeper layers, that may occur during sampling. The samples were stored in plastic bottles and frozen. Ashore they will be analysed for porosity, grain size, mineralogy and radionuclides content (^{234}Th, ^{137}Cs, ^{210}Pb).

The surface of the samples for X-ray was fixed by molten wax. The samples were stored at 4 °C and will be analysed by X-ray radiography in the laboratory ashore, in order to recognize physical properties and sedimentary structures of the cores.

Laboratories: ENEA-CRAM, ENEA-Brasimone

Thorium - 234

Thorium-234 has become a valuable tool for tracing scavenging processes over time-scales of days to weeks. Associated with POC profiles, thorium is used to quantify the sinking flux of organic carbon and other particle associated elements from the photic zone. Samples were collected by in situ pumping using battery-operated in situ pumps (Challenger Oceanics) that filter large volumes of water (100-1000 l) through a series of filters (Livingston and Cochran, 1987; Buesseler et al., 1992). Sea water samples were pumped sequentially through 10 µm Nitex screen (142 mm diameter), a 1-µm prefilter cartridge (24.5 cm length) to collect particulate matter and two MnO_2–impregnated cartridges (24.5 cm length) to extract dissolved ^{234}Th.

Suspended particulate matter collected on the Nitex screen was resuspended in 150 ml of filtered sea water by ultrasonication for 5 min, divided in subsamples on pre- combusted GF/F filters. The filters for thorium analysis were dried at 50°C and returned to laboratory where they were mounted on acrylic planchets and covered with a layer of plastic wrap and aluminium foil to shield low-energy beta particles. Beta emissions of ^{234}Pa, the high-energy beta-emitting daughter of ^{234}Th, were counted on a low-background RIS∅ gas-flow Geiger-Mueller counter operated in anti-coincidence mode. The filters and those for POC analysis was refrigerated at -18°C.

Cartridges will be dried and combusted at 500°C for 8-10 hours in the shore-based laboratory. Cartridge ash was analysed for ^{234}Th in counting jars with an ORTEC high purity Germanium detector. Gamma emission at 63.3 keV was corrected for the detector efficiency and decay-corrected to the midpoint of sample collection.

Laboratory: ENEA-CRAM, ENEA-Brasimone

Caesium – 137

Seawater samples were collected by the Rosette sampler. At the same time, salinity, temperature and dissolved oxygen concentration were measured by the CTD probe. After identification of the water masses by their hydrographic characteristics, samples of 60-100 l were collected, representative of MAW, LIW, WMDW. Caesium-137 was pre-concentrated onboard. The water was transferred in open polyethylene containers, and vigorously stirred; a known amount of ^{134}Cs was added as yield tracer; the pH was adjusted to 1.5, adding HCl to 37%. Then, 15 g of ammonium molybdophosphate (AMP) were suspended in 50 ml of distilled water and the suspension was added to the sample. Stirring was continued for 3-4 hours. The AMP was left to settle down for 6-8 hours.

The supernatant was discarded and the AMP was collected in a 5 l beaker. The walls of the container were washed with acidified distilled water (pH=1,5). The AMP in the beaker was left to settle, the supernatant was discarded and the AMP was transferred in a container for γ-spectrometry and dried in oven at 60°C. The activity will be measured on land by gamma spectrometry with high purity germanium detectors (30% relative efficiency, 1.7 keV resolution at 1332 keV).

Laboratory: ENEA-CRAM

Phytoplankton

Plankton net sampling at 100 m depth was performed. We used a 10 µm mesh net for phytoplankton. Samples were collected in dark bottles, and preserved with the addition of 8 ml of Lugol's solution. Quantification and classification of phytoplanktonic populations will be done in the laboratory ashore.

Laboratory: ENEA-CRAM

Mesopelagic fauna

Unlike surface fauna, mesopelagic fauna remains quite constant in space and time. They are extremely important in order to understand the trophic structure of the ecosystem, because they make up the natural reserve tapped by larger predators in a systematic or casual fashion when, for example, surface prey is scarce. These organisms were investigated in the water column through samplings using the Isaacs Kidd Midwater Trawl (IKMT). Detailed classification will be performed in the laboratory.

Laboratory: University of Genova

Solar spectra transmission (UV-VIS) and CDOM measurements

A submersible spectroradiometer (PUV 541, Biospherical Instruments) was used to measure upwelling and downwelling solar irradiance with depth in the water column (0-100m), at selected wavelengths (305 nm, 313 nm, 320 nm, 340 nm, PAR radiation). Sequentially, solar irradiance within the water column (0-30m) was measured using a spectroradiometer EPP2000C (StellarNet Inc., Tampa, FL, USA) able to operate in the wavelength range 290–800 nm (depth intervals of about 3 m with an uncertainty of 0.5 m). The spectral resolution was 3 nm, the instrument sensitivity was 10-4 Wm-2nm-1, and the measurements were made simultaneously with PUV 541 to inter-calibrate the spectral irradiance values. Each day, from 4 a. m. to 9 p. m., the solar irradiance at the water surface was measured using a 4 channels radiometer (Skye Instruments) positioned on the bow of the vessel. The radiometer measured the irradiance (according to the cosine law) at 381 nm, 441 nm, 589 nm and 681 nm with wavelength resolution of 12 nm, 10 nm, 10 nm and 12 nm respectively.

In collaboration with CNR-IBF group (using the identical experimental procedure), seawater samples for CDOM measurements were collected at different depths (surface to bottom). CDOM measurements will be carried out, in the laboratory ashore, with a Perkin Elmer Lambda 25 Spectrophotometer, equipped with 100 mm quartz cells, in 260-700 nm wavelength range.

Laboratory: Dpt. Chemical and Biosystem Sciences, University of Siena.

Preliminary Results

Hydrology

In the following pages are presented the first graphic elaborations of the CTD data (salinity, psu, potential temperature, °C, and dissolved oxygen, ml/l). An example of the results of the optical analysis is presented for station 905 in figure 19.

Potential temperature versus salinity plots are presented in figures 7 and 8. The stations were chosen in the middle of each transect. From the plots we can note different characteristics of the superficial layers (MAW), the intermediate layers (LIW) and the deep ones (WMDW). The highly saline intermediate water in the Sicily Strait (figure 7) is very evident and probably denotes the presence of Cretan Intermediate Water (CIW).

The circulation paths of the main water masses result clear from the vertical sections of the nine transects (figures 10-18). Arrows in the sections indicate the “complete stations”.

The **MAW** enters in the Ligurian Sea on the Corsica side and exists on the Ligurian side (figure 10). Then it moves toward the Gulf of Lions, where it enters from the eastern side (figure 11). In figure 13 we note the inflow of MAW from the Atlantic in the south, near Algeria, with low salinity values. The same flow we can see in the Sardinian Channel, on the south. MAW also occupies the whole transect in the Sicily Channel, with lower salinities on the Tunisian side, where it enters in the Eastern Mediterranean Sea. MAW reaches the Tyrrhenian Sea with a higher salinity (38.1-38.2), through the Sardinia-Sicily transect (figures 17 and 18).

LIW comes from the Eastern Mediterranean and is identified by a salinity and potential temperature maximum and, for his greater age, by an oxygen minimum. It enters in the Western Mediterranean Sea, through the Sicily Strait (figure 16), where it is visible at 150-250 m depth. After entering the western basin, it turns toward the Tyrrhenian Sea, through the Sardinia-Sicily transect (S>38.65, figures 17 and 18). LIW flows out from the Tyrrhenian Sea along the slope of Sardinia, as results clear observing the position of the salinity maximum in the Sardinian Channel (figure 15). The oxygen minimum is on the southern part, because it indicates the presence of a recirculated LIW, and therefore older, that returns towards the Tyrrhenian Sea. Looking at figure 14, it seems that the LIW that exits from the Tyrrhenian turns north, flowing along the western coast of Sardinia. In the Corsica-Liguria section, the LIW core seems to be located near the Ligurian coast (figure 10), according to the scheme proposed by Millot (1999), with the LIW coming from the Tyrrhenian Sea moves toward the Gulf of Lions, following the northern slope. Therefore, in the Gulf of Lions, the LIW vein enters from the east (figure 11) and is then involved in the convective processes of this dense water formation area.

The **WMDW** forms in the Gulf of Lions during winter. It has an anticlockwise circulation along the slope, round the whole Algero-Provençal Basin (figures 11, 12, 13). WMDW also moves from the Gulf of Lions towards the interior of the basin (figure 14), denoted by the deep high oxygen values (DO>4.75 ml/l). The Channel of Sardinia is a key place for the circulation of WMDW. It moves on the Tunisian side towards the Tyrrhenian Sea (figures 15 and 17). The bottom water in figure 16, indeed, comes from the Eastern Mediterranean Sea (Eastern Mediterranean Deep Water, **EMDW**) and is directed to the Tyrrhenian Sea.

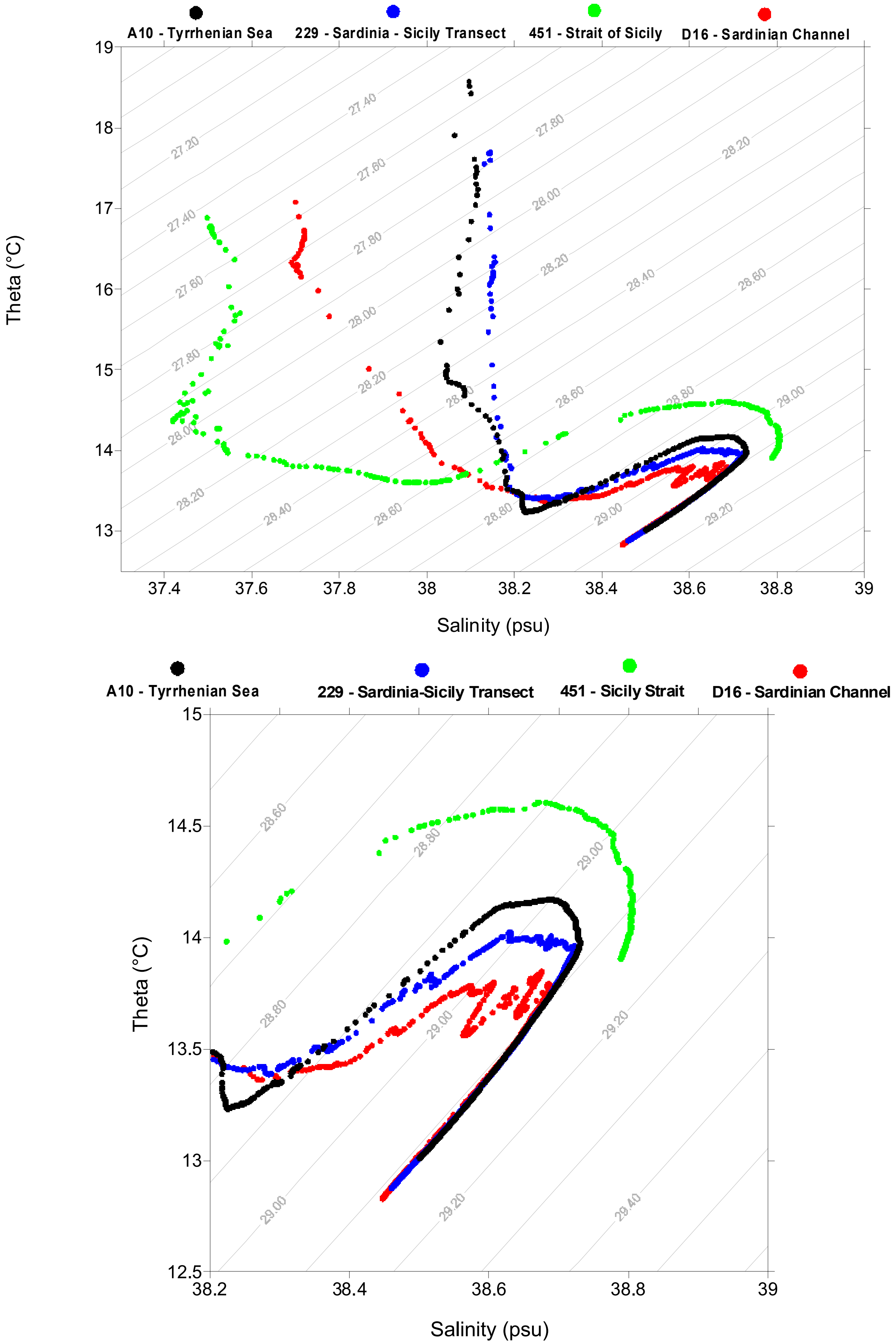

Figure 7 T-S plot of selected stations in the Central Mediterranean Sea and the Tyrrhenian Sea

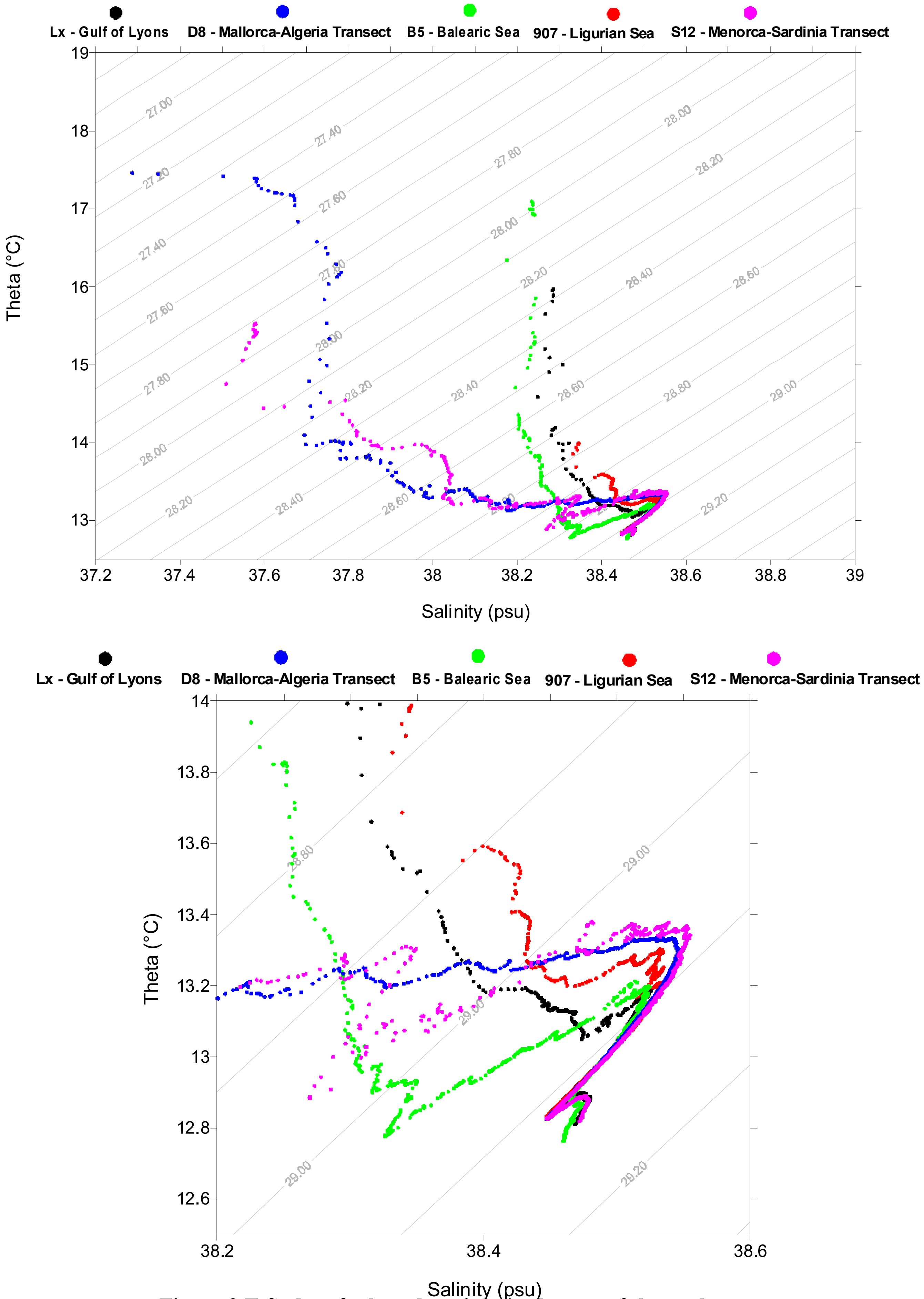

Figure 8 T-S plot of selected stations in the rest of the study area

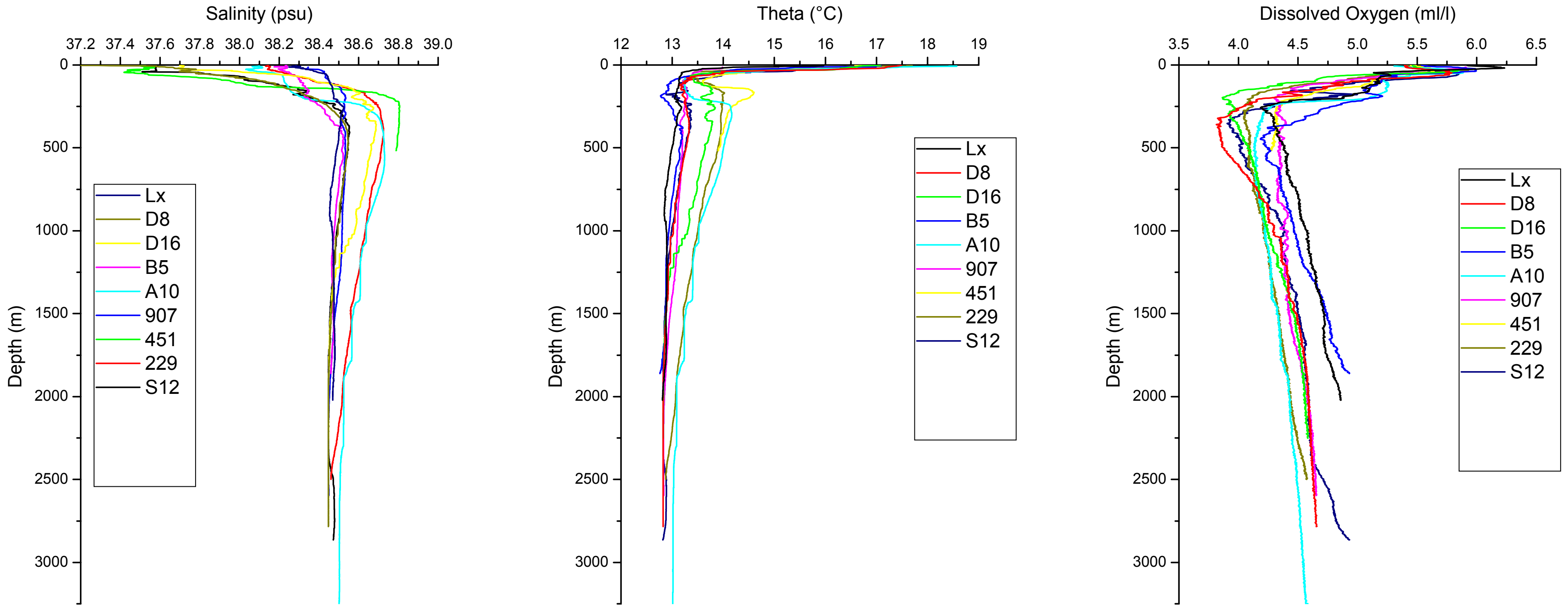

Figure 9 Vertical profiles for selected stations of salinity, potential temperature and dissolved oxygen

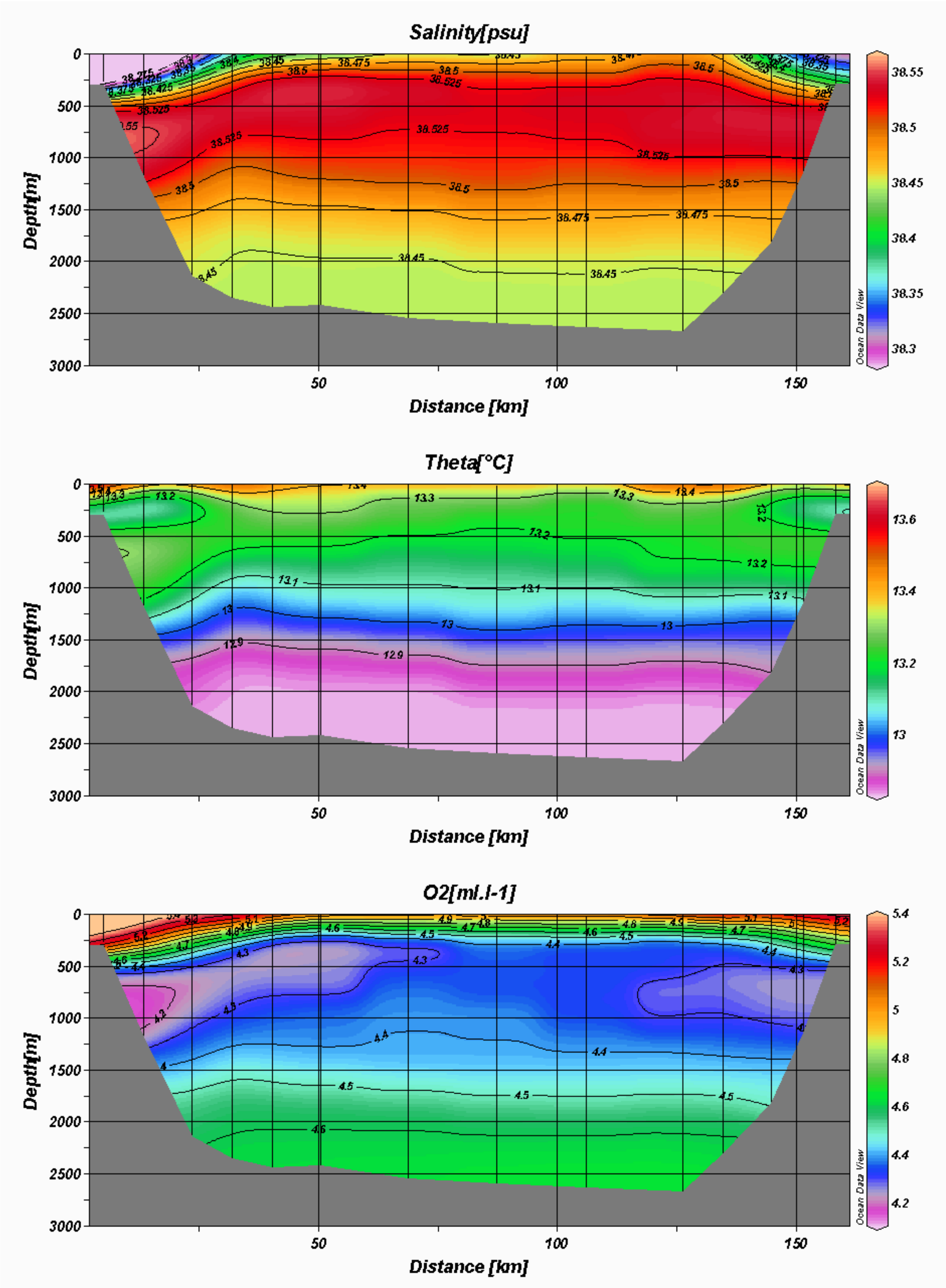

Figure 10 Corsica-Liguria Transect (Corsica on the right, Liguria on the left)

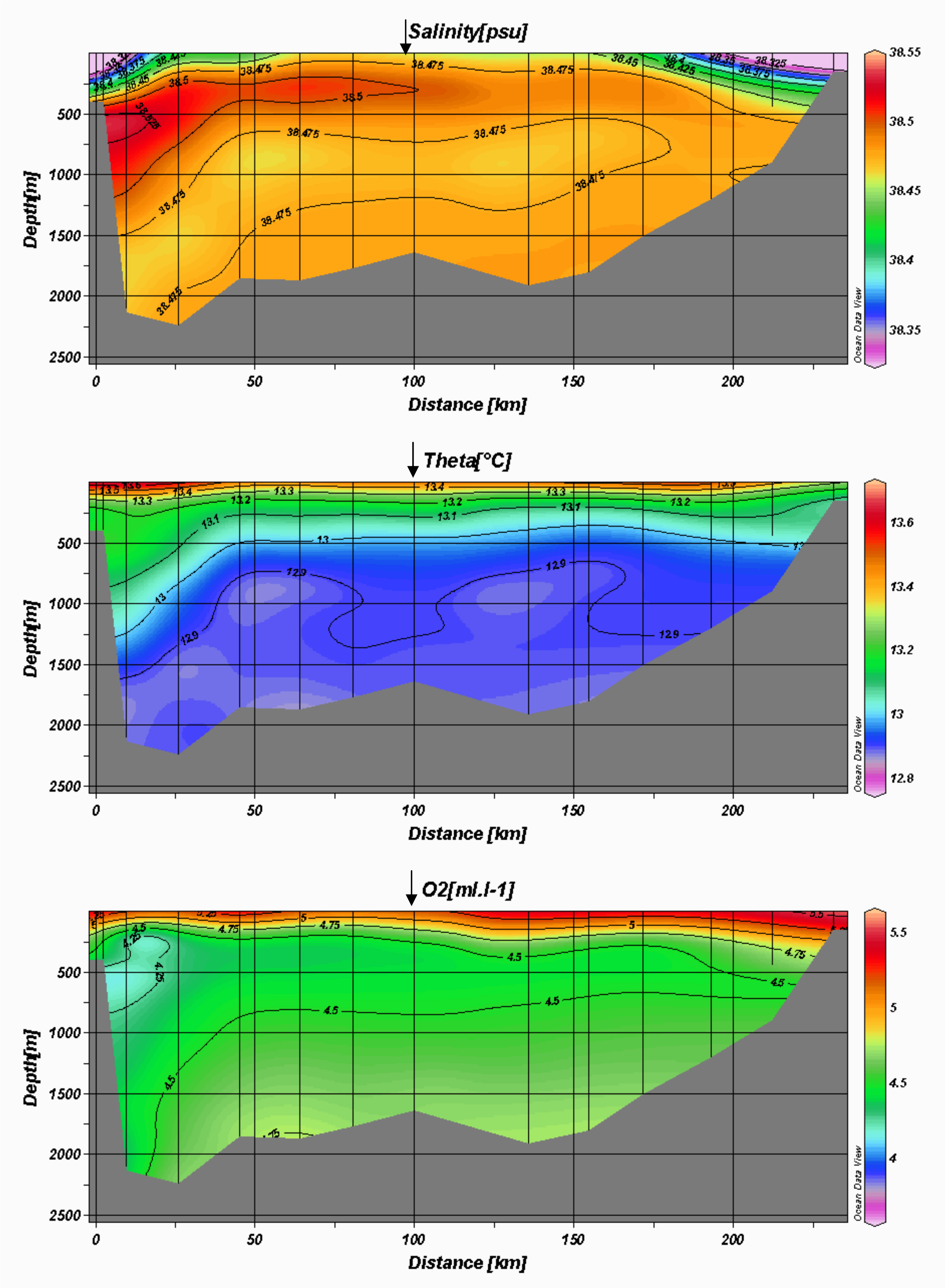

Figure 11 Gulf of Lions (west on the right, east on the left)

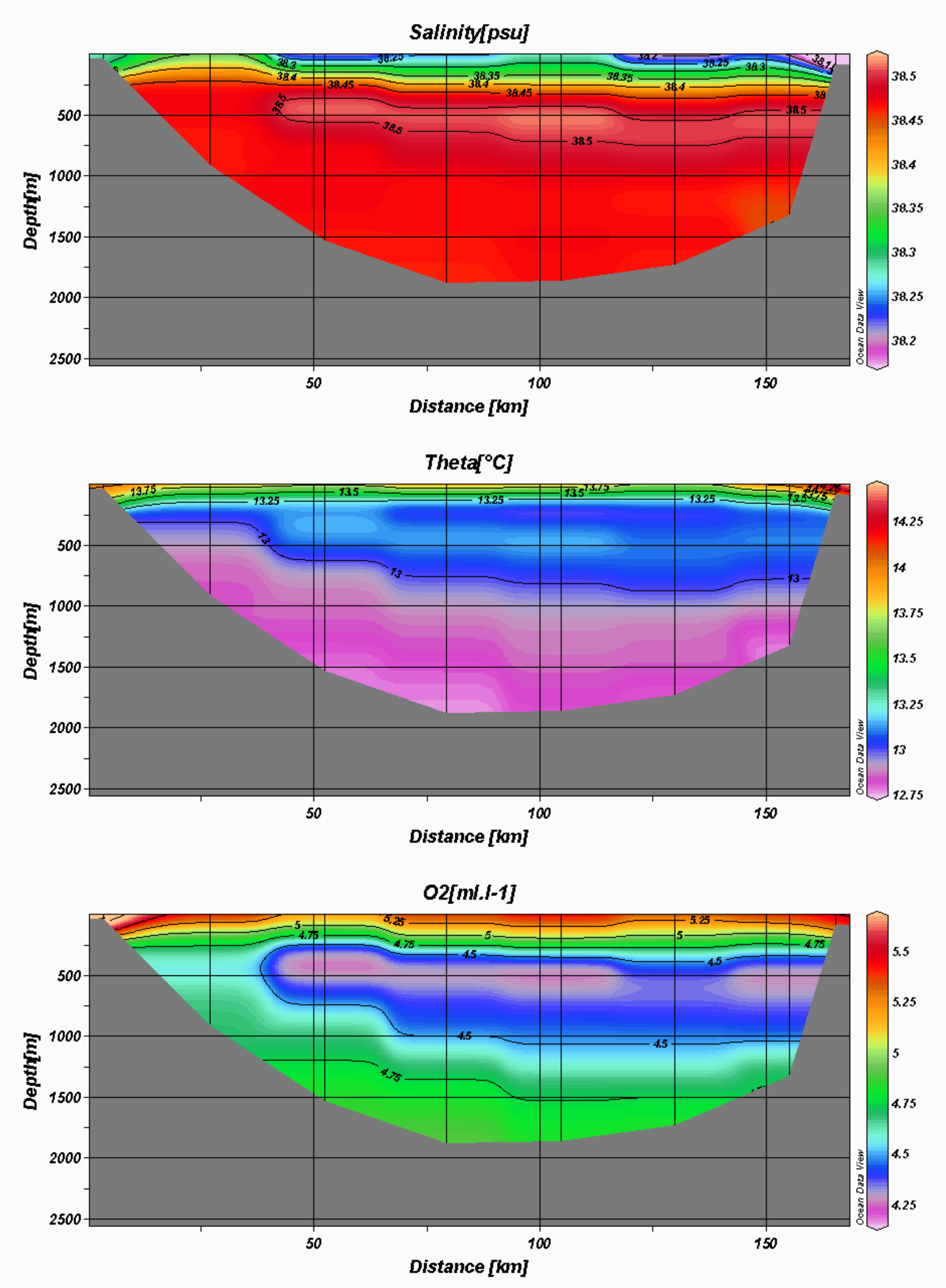

Figure 12 Balearic Sea (B1-B8) (south on the right, north on the left)

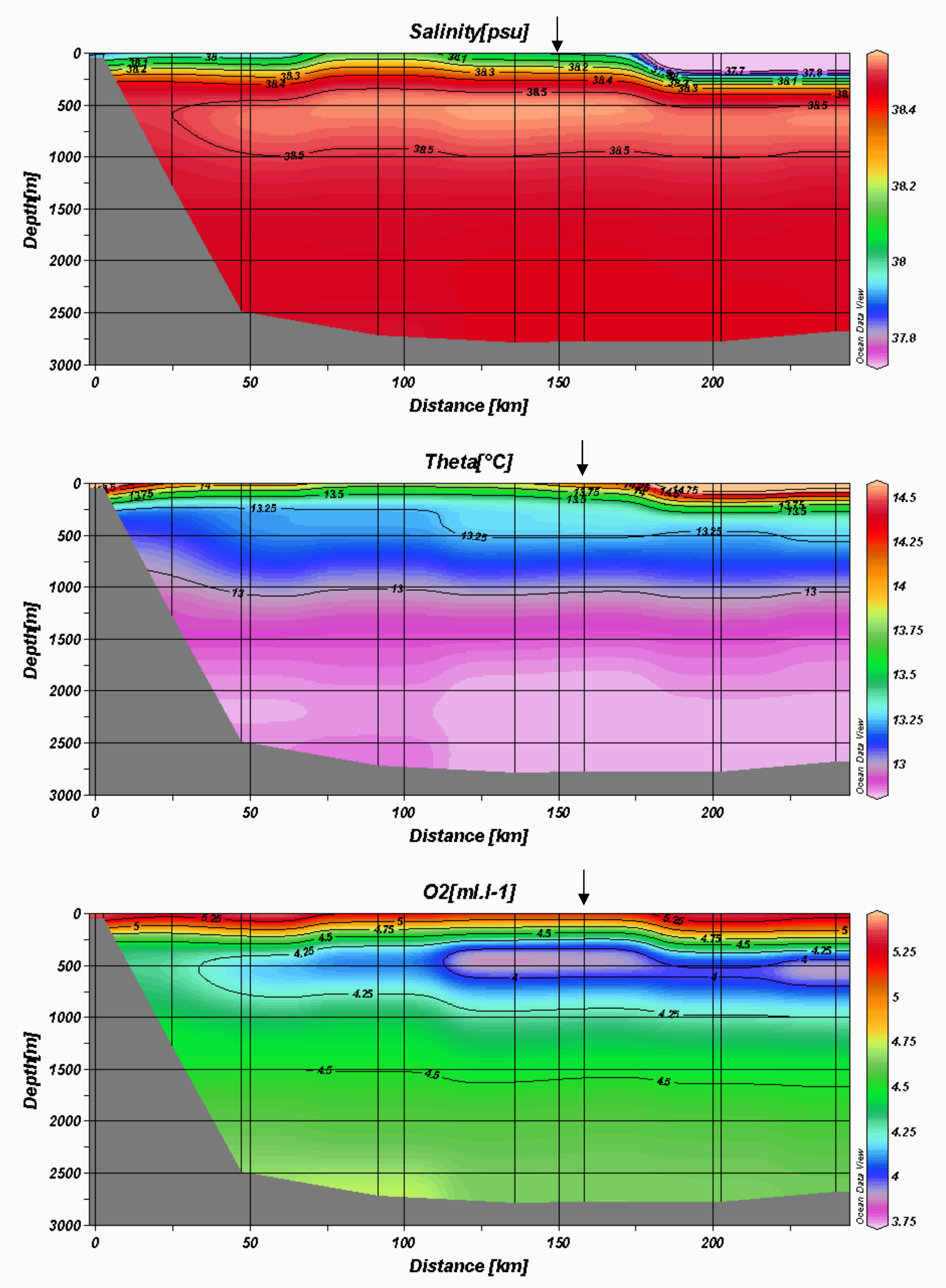

Figure 13 Mallorca-Algeria Transect (south on the right, north on the left)

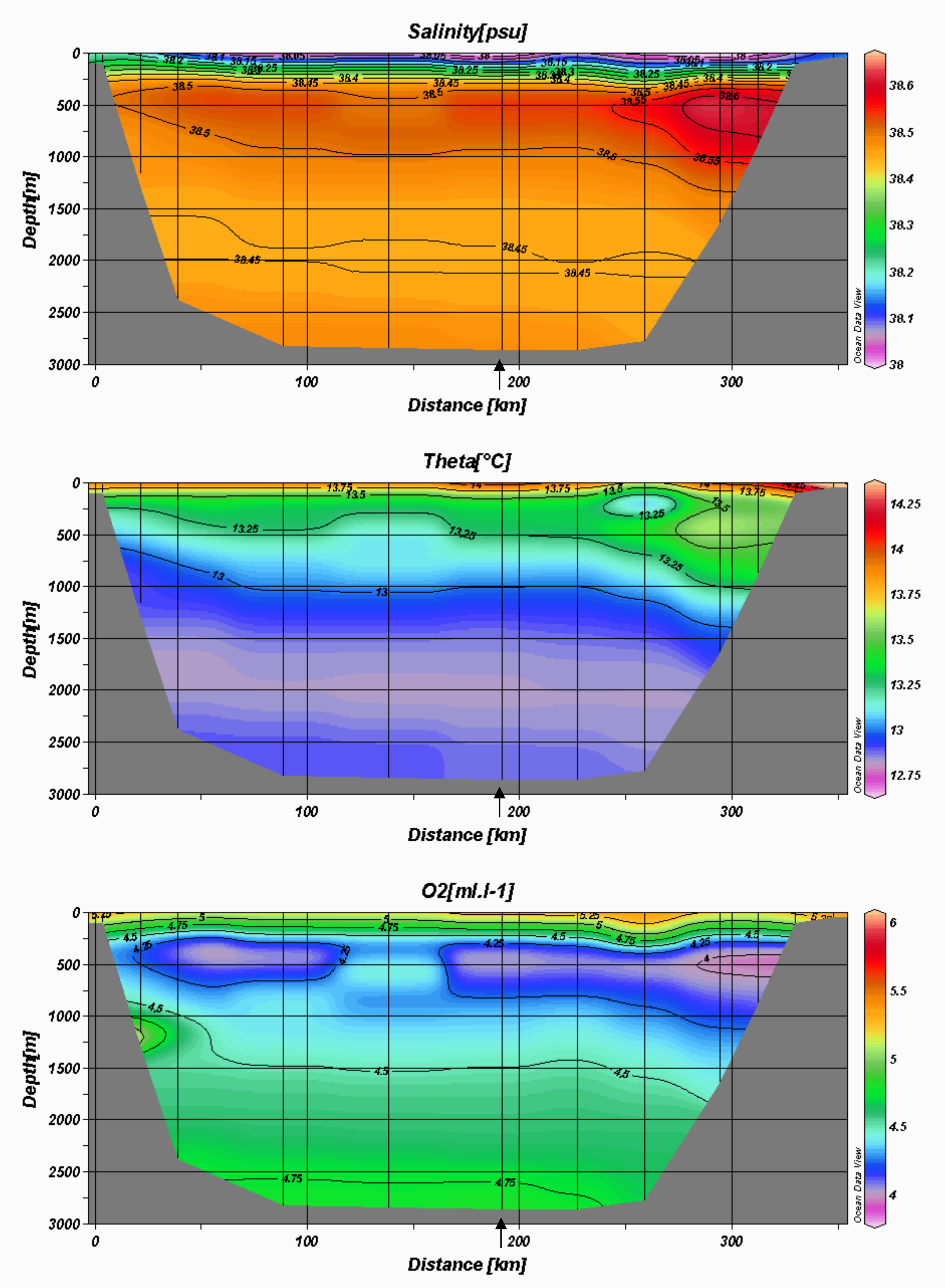

Figure 14 Menorca-Sardinia Transect (east on the right, west on the left)

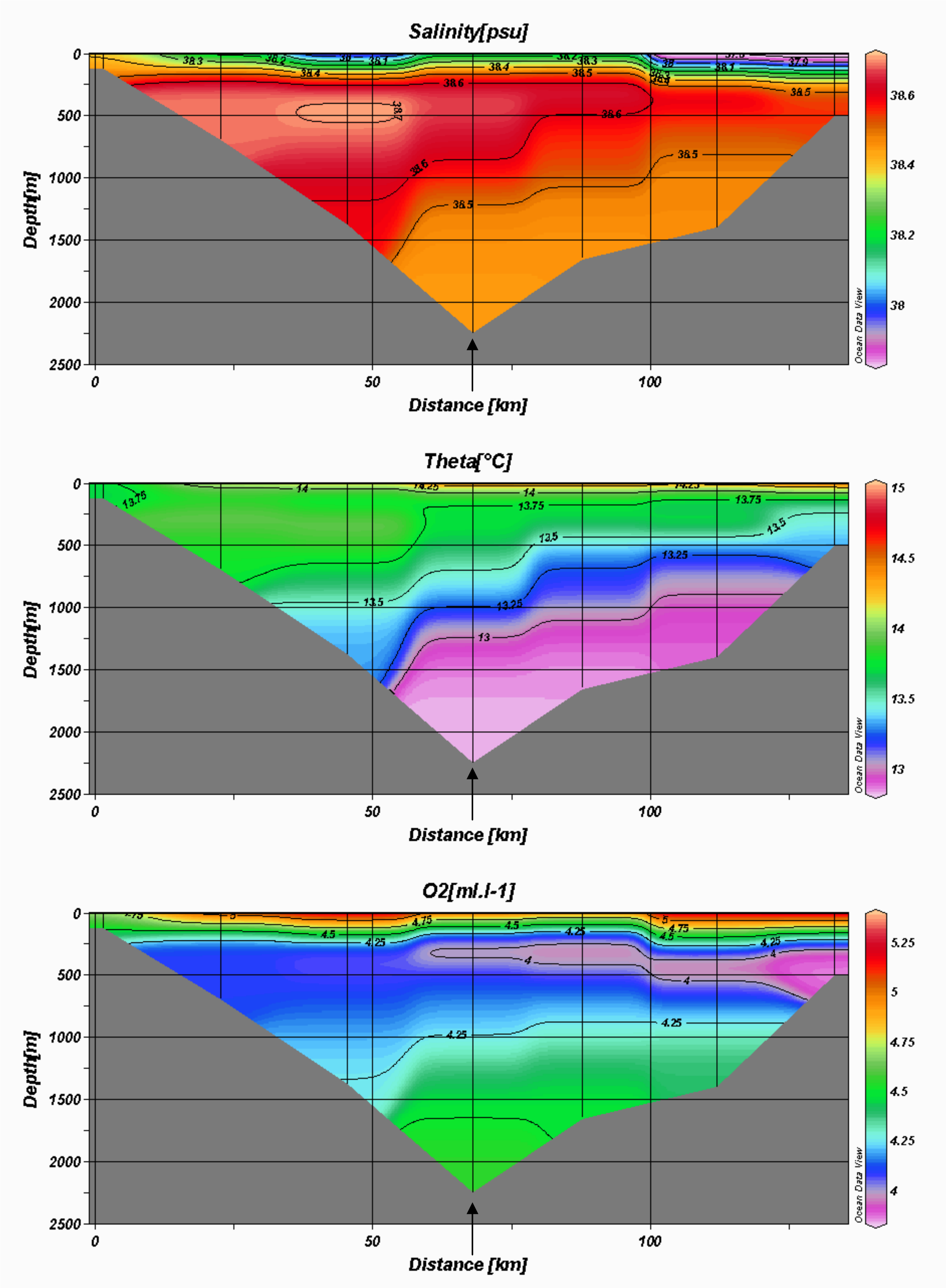

Figure 15 Sardinian Channel (south on the right, north on the left)

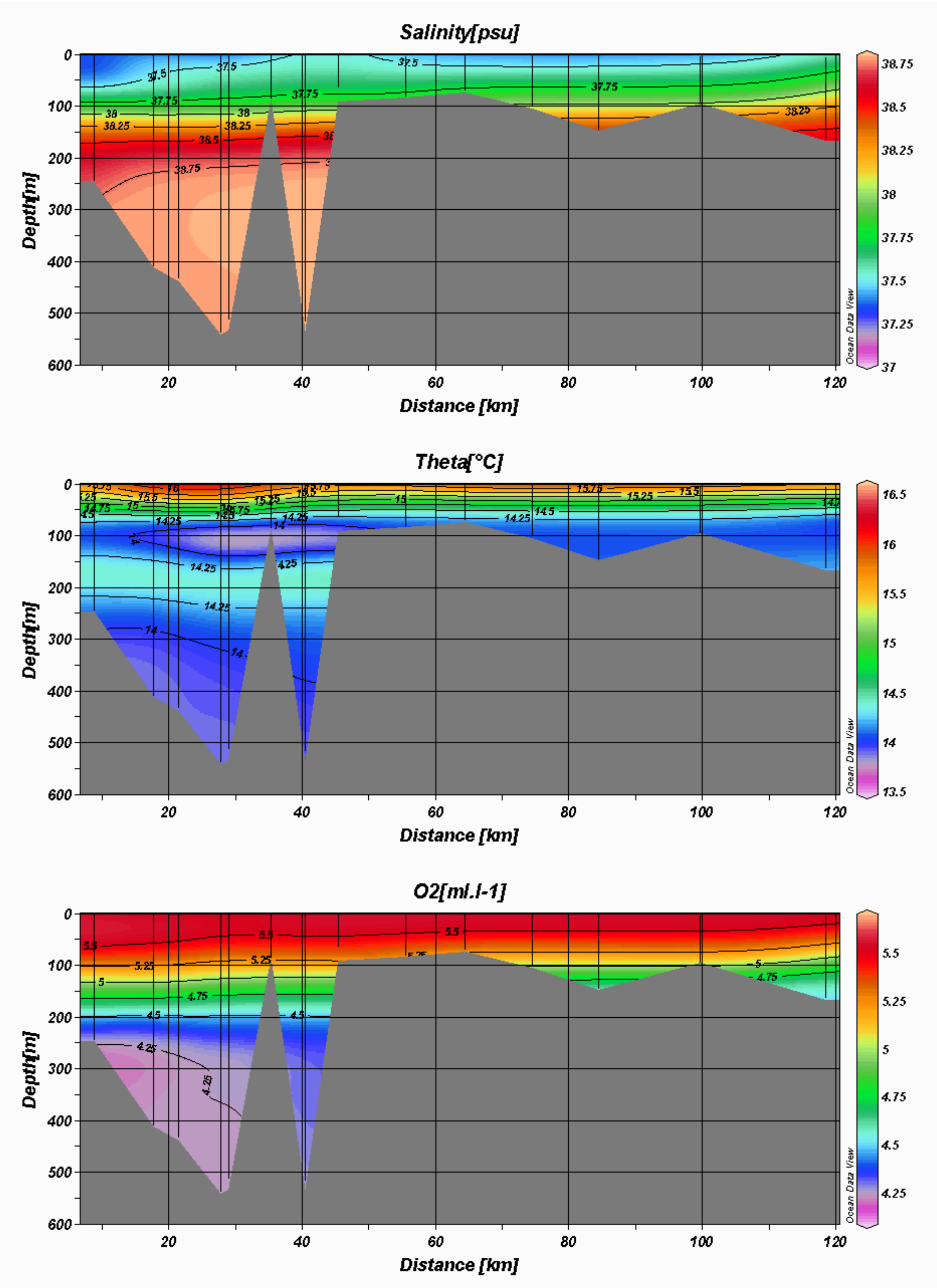

Figure 16 Sicily Channel (Sicily on the right, Tunis on the left)

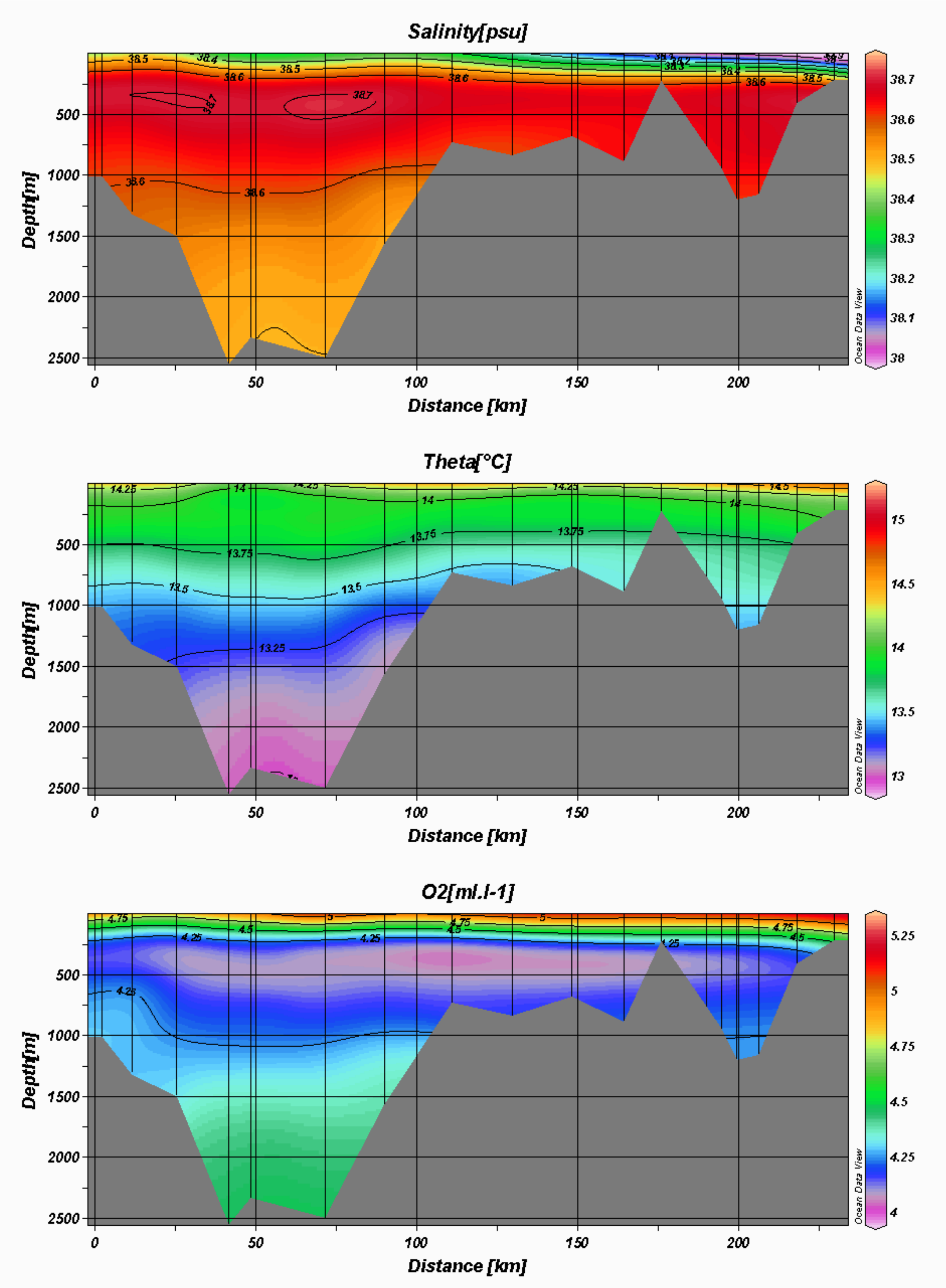

Figure 17 Sicily (on the right) – Sardinia (on the left) Transect

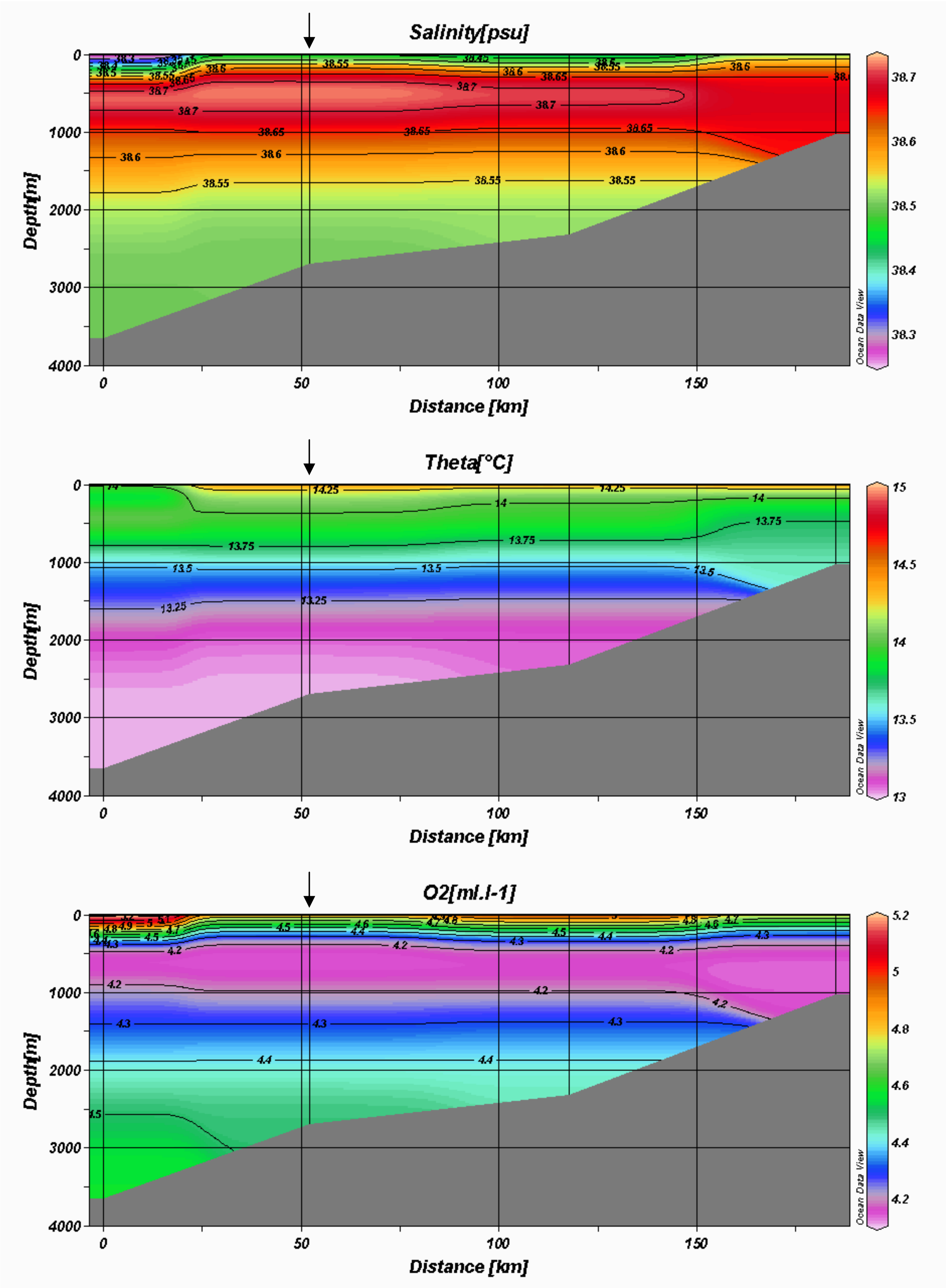

Figure 18 Tyrrhenian Sea (north on the right, south on the left)

Measurements of spectral attenuation of solar radiation in the water column

- Dattilo A. M. & Bracchini L., Dept. of Chemical and Biological Sciences, University of Siena -

Direct spectral measurements of the downward solar irradiance at different depths, in the visible (400-700 nm) and ultraviolet wavelengths (290-400 nm), were made using a spectroradiometer with spectral resolution of 3 nm (StellarNet). Irradiance values at the water surface were inter-calibrated by using a PUV 541 radiometer (measuring channel in 305 nm, 313 nm, 320 nm, 340 nm) and a Skye radiometer (measuring channel in 381 nm, 441 nm, 589 nm, 681 nm). In this section are shown the results obtained for station 905.

The changes in the spectral irradiance profiles with depth are shown in fig 19:

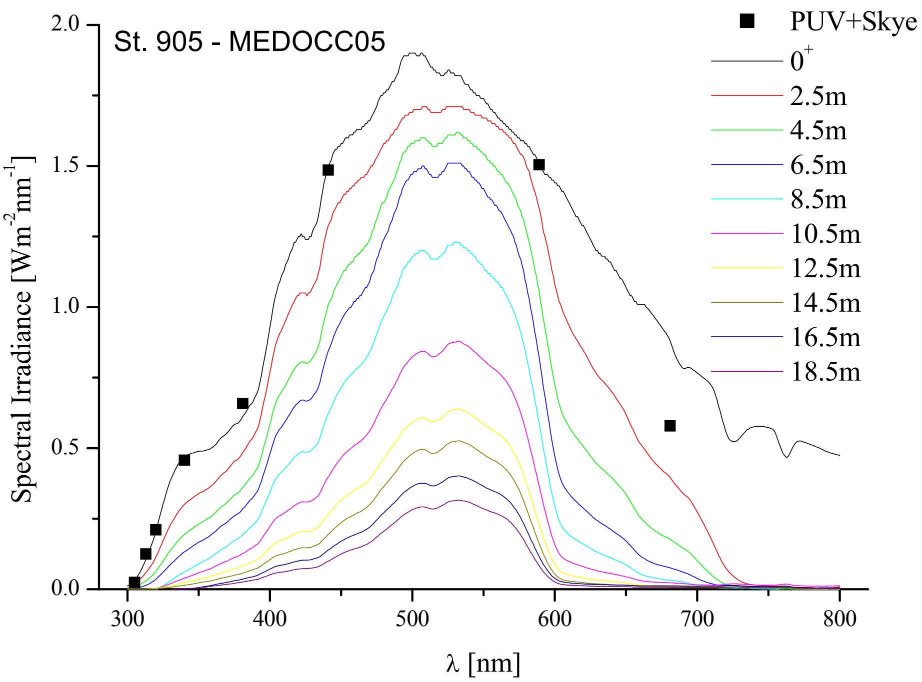

Figure 19 Spectral irradiance (Wm^{-2}nm^{-1}) as a function of wavelength (nm) in the first 18.5 m of the water column (St. 905). The black squares represent PUV 541 and Skye measurements at the water surface (0^{+}).

Solar irradiance upon water surface was characterised by a maximum value centred around 500 nm while a shift to values of about 530 nm occurred with increasing depths. The maximum irradiances values vary from 1.9 Wm^{-2}nm^{-1} (0^{+}) to 0.3 Wm^{-2}nm^{-1} (18.5 m). With increasing depths the spectral attenuation result very high in the 580-610 nm (absorption by water molecules). Applying the Lambert-Beer law to each wavelength, the spectral attenuation coefficients (K_λ) were calculated (Fig. 2).

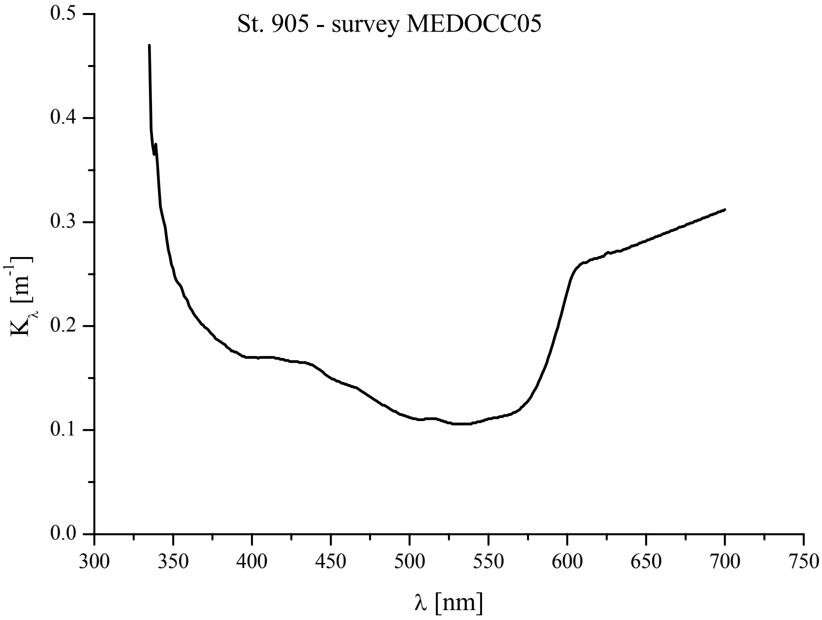

Figure 20 Spectral attenuation profile (m^{-1}) determined for the water mass between 2.5-18.5 m at St. 905.

A high increment of K_λ is present in the UVA and in the 580-610 nm wavebands (Fig. 20). Minimum attenuation values were observed in the visible spectra, between 500 nm and 550 nm. Values varied between 0.470 m^{-1} to 0.106 m^{-1}. In the transition UV-visible wavelengths (400 nm), K_λ has the value of 0.17 m^{-1}. The resulting penetration depths of solar radiation in the water column vary significantly (Fig. 21).

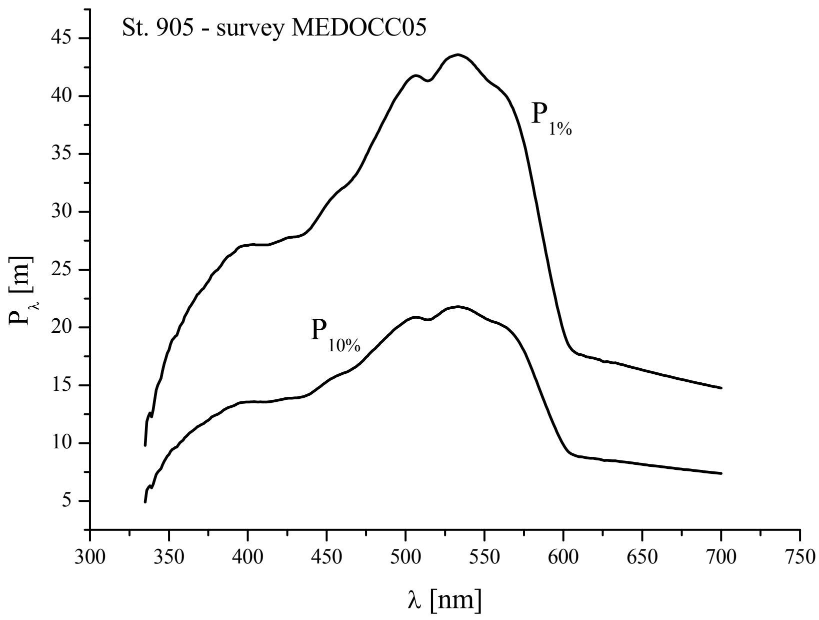

Figure 21 Penetration depths of 1% and 10% of the sub-surface irradiance values ($P_{1\%}$ and $P_{10\%}$) by wavelength.

UV irradiance (1%) was measured up to 27 m while the penetration depth of 10% was 13.5 m. In the visible wavelengths, $P_{1\%}$ maximum was 43-44 m (at 532-535 nm) and $P_{10\%}$ at 21-22 m. A plateau can be seen in the spectral attenuation in the blue region of the visible spectra (400-430 nm) (Fig. 2).

During the day, above surface measurements of broad-band irradiances were performed using Skye radiometers (UVA, UVB, Visible and PAR wavelength bands) (Fig. 22 and Fig. 23). The oscillation in the irradiance values were due to the presence of irregular cloud cover.

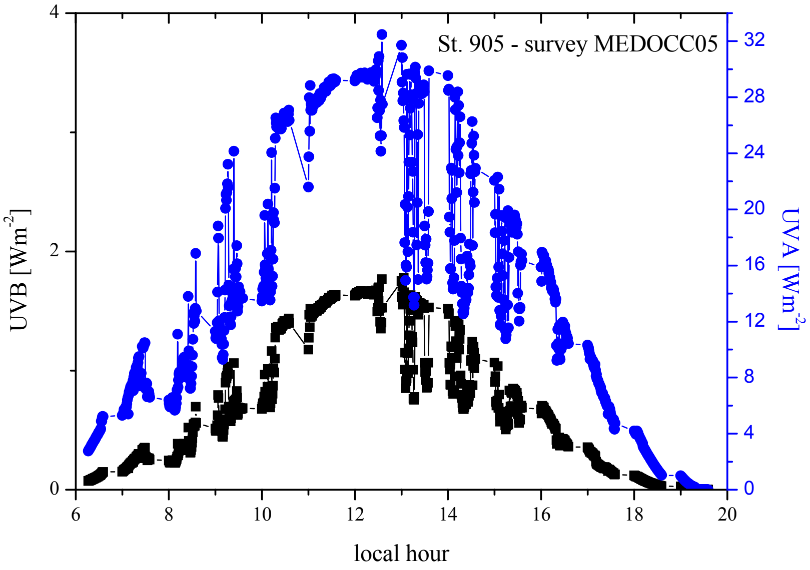

Figure 22 Above surface solar irradiance in the UVB and UVA bands (Wm^{-2}). The X-axis represents the local hour. Measured performed using a Skye radiometer positioned on the bow of the vessel.

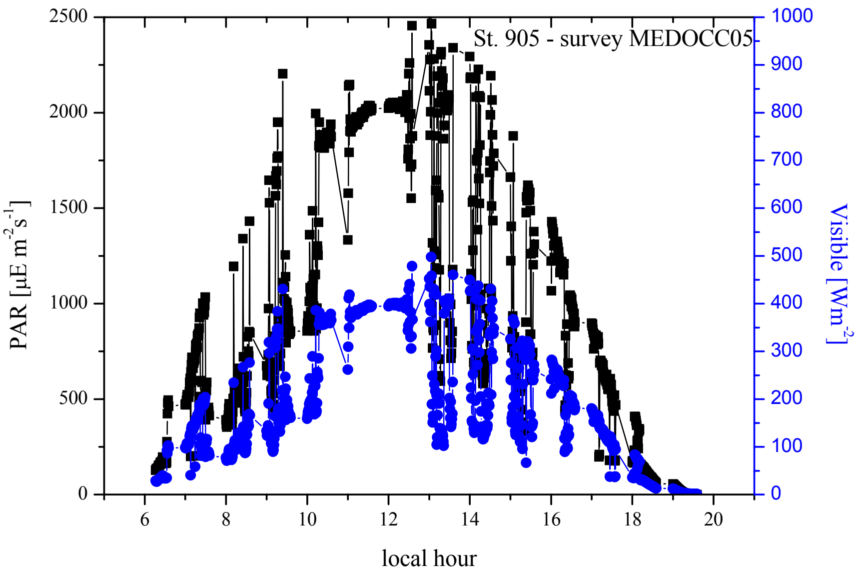

Figure 23 In-air PAR irradiance (µEm^{-2}s^{-1}) and visible irradiance (Wm^{-2}). The X-axis represents the local hour. Measured performed using a Skye radiometer positioned on the bow of the vessel.

The profile of Photosynthetic Active Radiation (PAR) irradiance (Fig. 24) did not follow a linear pathway (in a logarithm scale). An optical stratification of the surface layer of water mass (first 85±1 m) was seen (Fig. 25). Consequently, the surface water column was characterized by different values of PAR attenuation coefficients (Fig. 26). After 45±1 m the attenuation coefficients decrease rapidly than before 45±1 m (this is also clear from Fig. 24 in which the maximum curvature of the data points was showed after 40-45 m). 1% of sub surface PAR irradiance was found at a depth of 30±1 m, while 0.1% PAR was found at 50±1 m (Fig. 26).

The spectral irradiance at 313 nm (UV-B) was measured until 26.0±0.2 m (0.001 μWatt/cm^2 nm; Fig. 27). The depth at which it is possible measure this harmful irradiance is near the 1 % PAR irradiance depth (30 m). No optical stratification for this wavelength occurred and a single attenuation coefficient was found (0.36±0.01 m^{-1}). In the water column ultraviolet radiation is usually attenuated by chromophoric dissolved organic matter while PAR attenuation is driven largely by suspended solids (such as phytoplankton). Therefore, these results indicated that the superficial water column appears to be poorly mixed. The presence of suspended solid is likely to be higher in the first 45 meters with respect to the depth of 45-85 m. It appears that CDOM concentration, or its capacity to absorb ultraviolet radiation, in the first 26 m was constant.

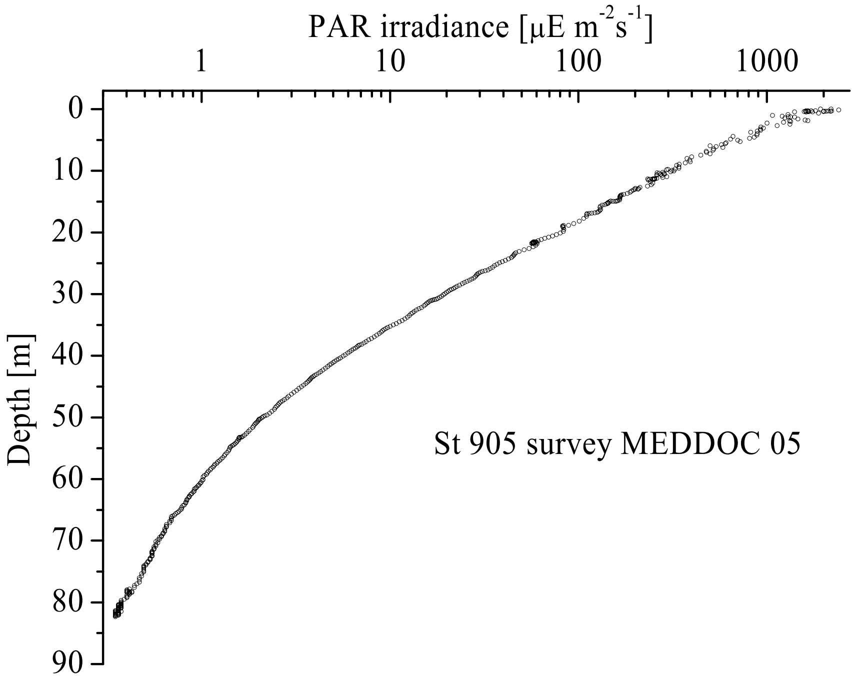

Figure 24 PAR irradiance profile (μEm^{-2}s^{-1}) vs. depth (m).

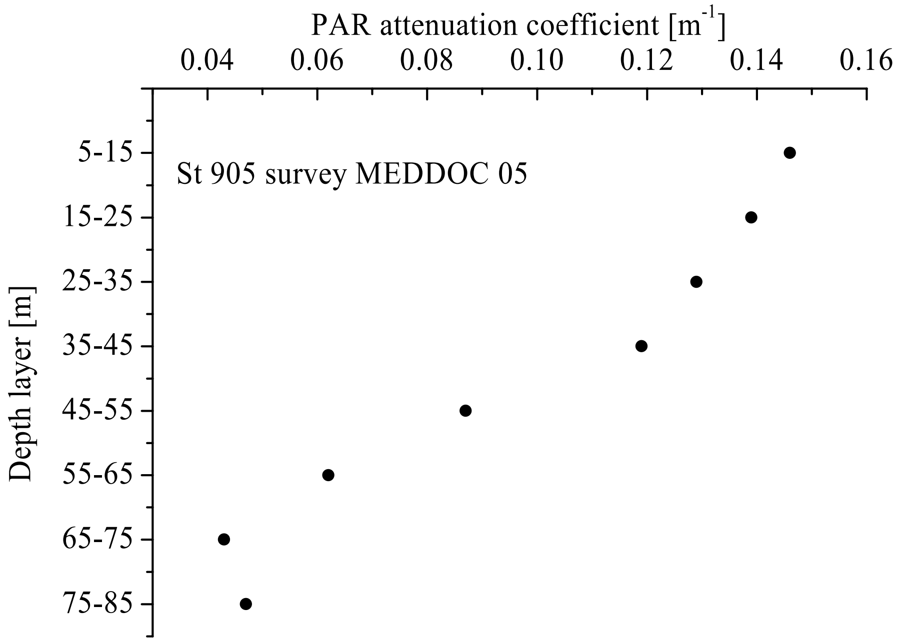

Figure 25 Attenuation coefficients in the PAR irradiance with depth layer.

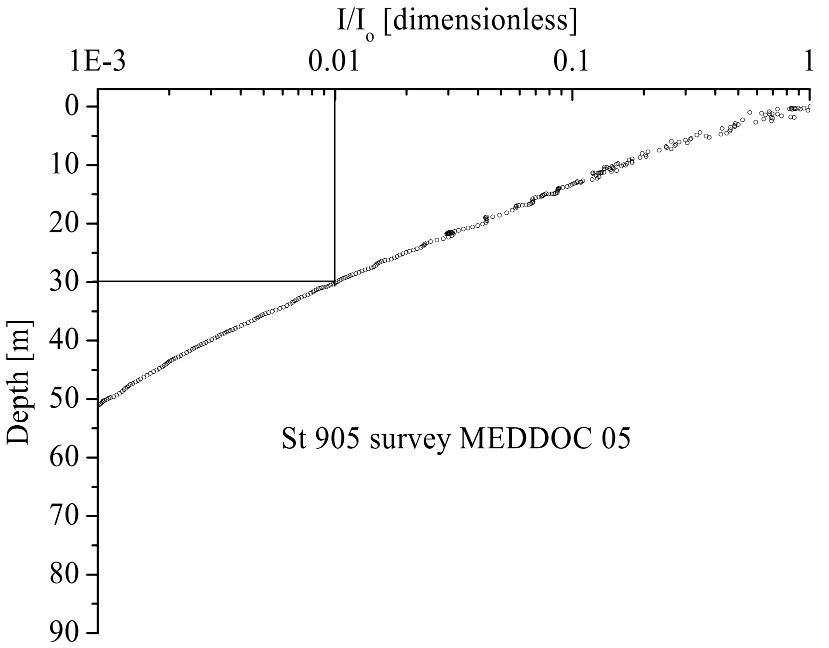

Figure 26 The ratio between measured PAR irradiance at sample depth (I) and the sub surface value (I_o)

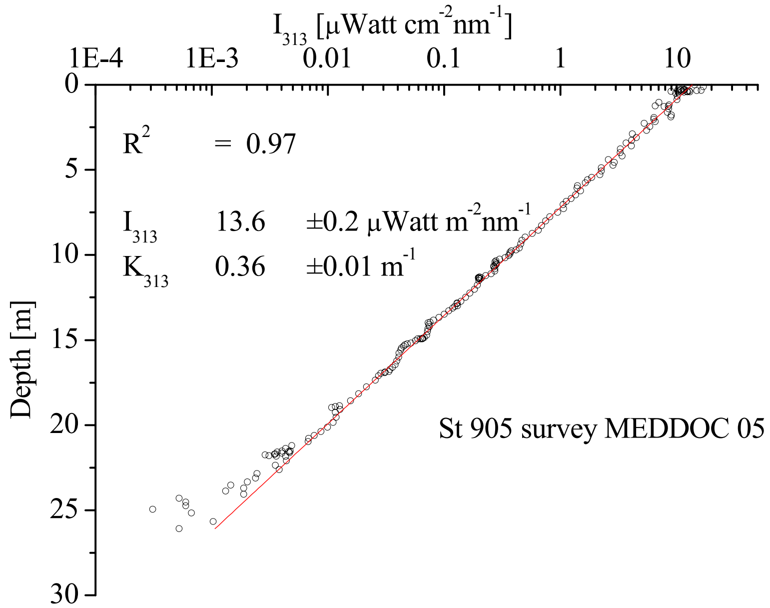

Figure 27 The 313 nm channel Irradiance profile (µW cm^{-2} nm^{-1}) vs. depth (m).

Acknowledgements

The scientific staff of MEDOCC 05 wishes to thank the Italian National Research Council (CNR), which made the R/V URANIA available for the cruise.
We also owe thanks to the Captain, the Officers and the Crew of the URANIA, without whose cooperation this work could not have been carried out.

References

- Astraldi M., Gasparini G. P., Vetrano A., Vignudelli S., 2002. Hydrographic characteristics and interannual variability of water masses in the central Mediterranean: a sensitivity test for long-term changes in the Mediterranean Sea. Deep-Sea Research I 49: 661–680.
- Astraldi M., Gasparini G.P., Sparnocchia S., Moretti S., Sansone M., 1996. The characteristics of the Mediterranean water masses and the water transport in the Sicily Channel at long time scales. In: Briand F. (Ed.), Dynamics of Straits and Channels, CIESM Science Series, Vol. 2, Monaco, pp. 95–118.
- Benzohra M., Millot C., 1995. Characteristics and circulation of the surface and intermediate water masses off Algeria. Deep Sea Res. 42 (10): 1803–1830.
- Buesseler K.O., Cochran J.K., Bacon M.P., Livingston H.D., Casso S.A., Hirschberg D., Hartman M.C., Fleer A.P., 1992. Determination of thorium isotopes in seawater by non-destructive and radiochemical procedures. Deep-Sea Research I 39, 1103-1114.
- Gasparini G. P., Zodiatis G., Astraldi M., Galli C., Sparnocchia S., 1999. Winter intermediate water lenses in the Ligurian Sea. Journal of Marine Systems 20: 319–332.
- Grasshoff K., Ehrhardt M., Kremling K., 1983. Methods of Seawater Analysis. Weinheim, Germany, Verlag Chemie.
- Hopkins T.S., 1988. Recent observations on the intermediate and deep water circulation in the Southern Tyrrhenian Sea. Oceanologica Acta 9: 41–50.
- Krivosheya V.G., Ovchinnikov I.M., 1973. Properties of the geostrophic circulation of the Tyrrhenian Sea. Oceanology 13: 822–827.
- Leaman K.D., Schott F.A., 1991. Hydrographic structure of the convection regime in the Gulf of Lions: winter 1987. J. Physical Oceanogr. 21 (4): 575–598.
- Livingston H.D., Cochran J.K., 1987. Determination of transuranic and thorium isotopes in ocean water: in solution and filterable particles. Journal of Radioanalytical and Nuclear Chemistry 115: 299-308.
- MEDOC Group, 1970. Observation of formation of deep water in the Mediterranean sea. Nature 227: 1037–1040.
- Millot C., 1985. Some features of the Algerian current. J. Geophys. Res. 90: 7169–7176.
- Millot C., 1999. Circulation in the Western Mediterranean Sea. Journal of Marine Systems 20: 423–442.
- Millot C., Benzhora M., Taupier-Letage I., 1997. Circulation in the Algerian Basin inferred from the MEDIPROD-5 currentmeters data. Deep-Sea Res. 44 (9/10): 1467–1495.

- Morel A., Andre J.M., 1991. Pigment distribution and primary production in the western Mediterranean as derived and modelled from Coastal Zone Color Scanner observations. J. Geophys. Res. 96: 12685–12698.
- Salat J., Font J., 1987. Water mass structure near and offshore the Catalan coast during the winters of 1982 and 1983. Annales Geophysicae 1B: 49–54.
- Santinelli C., Gasparini G. P., Nannicini L., Seritti A., 2002. Vertical distribution of dissolved organic carbon (DOC) in the Western Mediterranean Sea in relation to the hydrological characteristics. Deep-Sea Research I 49: 2203–2219.
- Sparnocchia S., Picco P., Manzella G.M.R., Ribotti A., Copello S., Brasey P., 1995. Intermediate water formation in the Ligurian Sea. Oceanol. Acta 12: 151–162.